

AD _____

GRANT NUMBER DAMD17-97-1-7014

TITLE: A New Invasion and Metastasis Molecule, Tiam1 and Its Interaction with the Cytoskeleton are Involved in Human Breast Cancer Progression

PRINCIPAL INVESTIGATOR: Lilly Y. Bourguignon, Ph.D.

CONTRACTING ORGANIZATION: University of Miami
Miami, Florida 33101

REPORT DATE: August 1998

TYPE OF REPORT: Annual

PREPARED FOR: U.S. Army Medical Research and Materiel Command
Fort Detrick, Maryland 21702-5012

DISTRIBUTION STATEMENT: Approved for Public Release;
Distribution Unlimited

The views, opinions and/or findings contained in this report are those of the author(s) and should not be construed as an official Department of the Army position, policy or decision unless so designated by other documentation.

DTIC QUALITY INSPECTED 4

19990713 126

REPORT DOCUMENTATION PAGE			Form Approved OMB No. 0704-0188	
Public reporting burden for this collection of information is estimated to average 1 hour per response, including the time for reviewing instructions, searching existing data sources, gathering and maintaining the data needed, and completing and reviewing the collection of information. Send comments regarding this burden estimate or any other aspect of this collection of information, including suggestions for reducing this burden, to Washington Headquarters Services, Directorate for Information Operations and Reports, 1215 Jefferson Davis Highway, Suite 1204, Arlington, VA 22202-4302, and to the Office of Management and Budget, Paperwork Reduction Project (0704-0188), Washington, DC 20503.				
1. AGENCY USE ONLY (Leave blank)		2. REPORT DATE August 1998		3. REPORT TYPE AND DATES COVERED Annual (7 Jul 97 - 6 Jul 98)
4. TITLE AND SUBTITLE A New Invasion and Metastasis Molecule, Tiam1 and Its Interaction with the Cytoskeleton are Involved in Human Breast Cancer Progression			5. FUNDING NUMBERS DAMD17-97-1-7014	
6. AUTHOR(S) Lilly Y. Bourguignon, Ph.D.				
7. PERFORMING ORGANIZATION NAME(S) AND ADDRESS(ES) Univesity of Miami Miami, Florida 33101			8. PERFORMING ORGANIZATION REPORT NUMBER	
9. SPONSORING / MONITORING AGENCY NAME(S) AND ADDRESS(ES) U.S. Army Medical Research and Materiel Command Fort Detrick, Maryland 21702-5012			10. SPONSORING / MONITORING AGENCY REPORT NUMBER	
11. SUPPLEMENTARY NOTES				
12a. DISTRIBUTION / AVAILABILITY STATEMENT Approved for Public Release; Distribution Unlimited			12b. DISTRIBUTION CODE	
13. ABSTRACT (Maximum 200 words) <p>In this study we have examined the interaction between the guanine nucleotide exchange factor, Tiam1, and the cytoskeletal protein, ankyrin, in metastatic breast cancer cells (Met-1 cell line). Immunoblot assay using anti-Tiam1-specific antibody shows that Tiam1 is a 200 kDa polypeptide in Met-1 cells. Structural analysis indicates that the amino acid sequence, "717GEGTDAVKRS727L", in Tiam1 shares a great deal of structural homology with the ankyrin-binding domain located in CD44 isoforms. Most importantly, we have determined that ankyrin binding to Tiam1 activates GDP-GTP exchange on RhoA. In addition, overexpression of Tiam1 (by transfecting Met-1 cell with Tiam1 cDNAs) induces ankyrin-linked cytoskeletal changes and membrane motility (e.g. membrane spikes and ruffling), tumor cell invasion and migration. Finally, we have constructed a Tiam1 deletion mutant lacking the ankyrin binding site. This truncated cDNA was then transiently transfected into Met-1 cells. Our results indicate that this Tiam1 deletion mutant (lacking an ankyrin binding and displaying a reduced GDP-GTP exchange activity for RhoA) functions as a potent dominant-negative form of Tiam1 which effectively inhibits metastatic tumor cell behaviors. These findings strongly suggest that the ankyrin binding site located within Tiam1 plays a pivotal role in RhoA activation required for ankyrin-based cytoskeleton function and oncogenic signaling (e.g. membrane motility, tumor cell invasion and migration) during metastatic breast tumor cell progression.</p>				
14. SUBJECT TERMS Breast Cancer			15. NUMBER OF PAGES 31	
			16. PRICE CODE	
17. SECURITY CLASSIFICATION OF REPORT Unclassified	18. SECURITY CLASSIFICATION OF THIS PAGE Unclassified	19. SECURITY CLASSIFICATION OF ABSTRACT Unclassified	20. LIMITATION OF ABSTRACT Unlimited	

FOREWORD

Opinions, interpretations, conclusions and recommendations are those of the author and are not necessarily endorsed by the U.S. Army.

L.B. Where copyrighted material is quoted, permission has been obtained to use such material.

L.B. Where material from documents designated for limited distribution is quoted, permission has been obtained to use the material.

L.B. Citations of commercial organizations and trade names in this report do not constitute an official Department of Army endorsement or approval of the products or services of these organizations.

L.B. In conducting research using animals, the investigator(s) adhered to the "Guide for the Care and Use of Laboratory Animals," prepared by the Committee on Care and use of Laboratory Animals of the Institute of Laboratory Resources, national Research Council (NIH Publication No. 86-23, Revised 1985).

L.B. For the protection of human subjects, the investigator(s) adhered to policies of applicable Federal Law 45 CFR 46.

L.B. In conducting research utilizing recombinant DNA technology, the investigator(s) adhered to current guidelines promulgated by the National Institutes of Health.

L.B. In the conduct of research utilizing recombinant DNA, the investigator(s) adhered to the NIH Guidelines for Research Involving Recombinant DNA Molecules.

L.B. In the conduct of research involving hazardous organisms, the investigator(s) adhered to the CDC-NIH Guide for Biosafety in Microbiological and Biomedical Laboratories.

Willy G. W. Bungen
PI - Signature

Date

10/22/98

TABLE OF CONTENTS

	<i>Page Number</i>
FRONT COVER	1
REPORT DOCUMENTATION PAGE SF 298.....	2
FOREWORD	3
TABLE OF CONTENTS	4
INTRODUCTION	5
BODY	6-13
CONCLUSIONS	14-16
REFERENCES	16-18
APPENDICES	19-31

(5) INTRODUCTION

CD44 isoforms belong to a family of transmembrane glycoproteins which are widely distributed in different cells and tissues (1-7). They include CD44s (the standard form), CD44E (the epithelial form) and CD44v (variant isoforms) arise from differential splicing of one to ten (or eleven) variable exons that encode portions of the membrane proximal extracellular domain (8). The molecular diversity of CD44 isoforms is further compounded by differential biosynthetic processes and post-translational modifications [e.g. N-/O-glycosylation (9-12) or glycosaminoglycan (GAG) addition] (13,14). This structural arrangement, which occurs within either the invariant region or the extracellular domain of the variant region, is important for CD44-mediated communication between extracellular matrix components and intracellular protein components (e.g. cytoskeletal proteins and various regulatory enzymes) (6,7,9,15-23). The 15 amino acid sequence [e.g. NSGNQAVEDRKPSGL (in human) (21) or NGNGTVEDRKPSSEL (in mouse) (20)] residing in the cytoplasmic domain of CD44 isoforms is the ankyrin-binding domain of this family of transmembrane glycoproteins. Biochemical analyses plus in vitro mutagenesis indicate that the ankyrin-binding domain is required for CD44-mediated "outside-in" and "inside-out" cell signaling (6,7,20,21). Moreover, the transmembrane linkage between CD44v isoforms and the cytoskeleton promotes invasive and metastatic-specific tumor phenotypes [e.g. matrix degradation (MMPs) activities, "invadopodia" formation (membrane projections), tumor cell invasion and migration] (24). These findings strongly suggest that the interaction between CD44 isoforms and the cytoskeleton plays a pivotal role in the onset of oncogenesis and tumor progression.

Members of the Rho subclass of the ras superfamily [small molecular weight GTPases, (e.g. RhoA, Rac1 and Cdc42)] are known to be associated with changes in the membrane-linked cytoskeleton (25,26). For example, activation of RhoA, Rac1 and Cdc42 have been shown to produce specific structural changes in the plasma membrane-cytoskeleton associated with membrane ruffling, lamellipodia, filopodia, and stress fiber formation (25,26). The coordinated activation of these GTPases is considered to be a possible mechanism underlying cell motility, an obvious prerequisite for metastasis (27-29). Tsukita and his co-workers have reported that Rho-like proteins participate in the interaction between the CD44 and the ERM cytoskeletal proteins (26). Our recent study also supports the notion that RhoA-activated Rho-kinase (ROK) plays an important role in regulating CD44v_{3,8-10}-specific metastatic behaviors in breast tumor cells such as Met-1 cells (30). Consequently, it would be important to search for the upstream activator(s) for RhoA during CD44v_{3,8-10}-related oncogenic signaling.

Several guanine nucleotide exchange factors (GEFs - the db1 or DH family) have been identified as oncogenes due to their ability to up-regulate RhoGTPase activity leading to malignant transformation (31). One of these GEFs is Tiam1 (T lymphoma invasion and metastasis) which was identified by retroviral insertional mutagenesis and selection for invasive cells in vitro (32,33). This molecule is largely hydrophilic and, by sequence homology, contains numerous functional domains found in signal transduction proteins (3,4). For example, the C-terminal region of the Tiam1 molecule contains a Db1 homology (DH) domain (34,35) and an adjacent pleckstrin homology (PH) domain which are commonly detected in most GEFs (36). In particular, the DH domain of these proteins exhibits GDP/GTP exchange activity for specific members of the Ras superfamily of GTP-binding proteins (34,35). Tiam1 also contains an additional PH domain, a Discs-large homology region (DHR) (37) and a potential myristoylation site in the N-terminal part of the protein (32).

Overexpression of both N- and C-terminally truncated, as well as full-length, Tiam1 proteins induces the invasive phenotype in otherwise noninvasive lymphoma cell lines (32). Moreover, such invasive cell behavior correlates with metastasis in animal models (32). It is also well-established that Tiam1 is capable of activating RhoA and Rac1 in vitro as a GEF and induces membrane cytoskeleton-mediated cell shape changes, cell adhesion and cell motility (38-41). These findings have prompted several research groups to investigate the mechanisms involved in the regulation of Tiam1. For example, Tiam1 has been shown

to become phosphorylated by protein kinase C (PKC) in Swiss 3T3 fibroblasts stimulated by lysophosphatidic acid (LPA) (42) and platelet-derived growth factor (PDGF) (43). Addition of serum to NIH3T3 cells transfected with N-terminally truncated Tiam1 induces Tiam1 association with membranes (44). Although a Tiam1 transcript has been detected in breast cancer cells (33), it was not clear whether it functions as a GEF in activating Rho-like GTPases; and how this molecule is regulated in invasive and metastatic processes of breast cancer cells.

In this study we have examined the expression of Tiam1 in CD44v_{3,8-10} containing metastatic breast tumor cells (Met-1 cell line) using immunological techniques. Biochemical analyses show that Tiam1 contains an ankyrin-binding domain similar to that detected in CD44, and that ankyrin binding to Tiam1 activates Tiam1-RhoA signaling. Overexpression of Tiam1 in Met-1 cells by transfecting Tiam1 cDNA induces cytoskeleton and CD44v_{3,8-10}-associated metastatic phenotypes (e.g. membrane motility, tumor cell invasion and migration). This tumor cell behavior can be effectively blocked by transfecting Met-1 cells with a Tiam1 deletion mutant (lacking an ankyrin-binding domain) cDNA or certain agents [e.g. CD44 antibodies or the RhoA inhibitor, C3-toxin]. These findings suggest that ankyrin binding to Tiam1 plays a pivotal role in regulating RhoA signaling required for CD44v_{3,8-10}-associated cytoskeleton functions (e.g. membrane motility and tumor cell migration) during metastatic breast tumor cell progression.

(6) BODY

MATERIALS AND METHODS

Cell Culture: Mammary tumor cells containing the polyoma virus middle T (PyV-MT) transgene under the transcriptional control of the MMTV LTR promoter were used to initiate a transplantable line in nude mice. The PyV-MT transgenic mammary tumor cells were obtained from mammary tumors which arose in the transgenic colony at the Institute for Molecular Biology and Biotechnology, McMaster University, Hamilton, Ontario, Canada (Dr. William J. Muller). Mammary tumors were collagenase/dispase (Worthington, Freehold, N. J.) treated, and 5 x 10⁵ cells per 100µl were transplanted subcutaneously as a bolus via syringe and a 25 gauge needle into the thoracic region of nude mice. The resulting high potential metastatic PyV-MT transgenic mammary tumor line, Met-1, was maintained by serial transplantation of 1 mm³ tumor segments into either subcutaneous tissue (ectopic) or intact mammary fat pads (orthotopic).

The Met-1 tumor line was dissociated after transplant generation one and plated onto T-75 flasks to develop a tissue culture line (45). The Met-1 cell line was cultured in high glucose DMEM supplemented by 10% fetal bovine serum, 2mM glutamine, and antibiotics (Sigma, St Louis, MO). The Met-1 cell line is currently in passage 30.

COS-7 cells were obtained from American Type Culture Collection and grown routinely in Dulbecco's Modified Eagle's Medium (DMEM) containing 10% fetal bovine serum, 1% glutamine, 1% penicillin and 1% streptomycin.

Antibodies and Reagents: Monoclonal rat anti-human CD44 antibody (Clone:020; Isotype: IgG_{2b}; obtained from CMB-TECH, Inc., Miami, FL.) used in this study recognizes a common determinant of the CD44 class of glycoproteins including CD44s and other variant isoforms (46) and is capable of precipitating all CD44 variants. For the preparation of polyclonal rabbit anti-CD44v3 or rabbit anti-Tiam1 antibody, specific synthetic peptides [≈15-17 amino acids unique for either CD44v3 or the C-terminal sequence of Tiam1] were prepared by the Peptide Laboratories of Department of Biochemistry and Molecular Biology using an Advanced Chemtech automatic synthesizer (model ACT350). These peptides (e.g. CD44v3 or Tiam1) were conjugated to polylysine and subsequently injected into rabbits to raise the antibodies. The anti-CD44v3 or anti-Tiam1-specific antibody was collected from each bleed and stored at 4°C containing 0.1% azide.

Both anti-CD44v3 and the anti-Tiam1 IgG fraction were prepared by conventional DEAE-cellulose chromatography, respectively. Mouse monoclonal anti-HA (hemagglutinin epitope) antibody (clone 12 CA5) was purchased from Boehringer

Mannheim. Clostridium botulinum C3 toxin was obtained from List Biological Laboratories, Inc. Escherichia coli (E. coli)-derived GST-tagged RhoA was a gift from Dr. Martin Schwartz (Scripps Research Institute, La Jolla, CA).

Microinjection of the RhoA inhibitor, C3 toxin into Met-1 cells:

Met-1 cells were plated onto glass coverlips and cultured in high glucose DMEM supplemented by 10% fetal bovine serum and 2mM glutamine. C3 toxin (50µg/ml) [in a microinjection buffer containing 50mM Hepes (pH 7.2), 100mM KCl, 5mM NaHPO₄ (pH 7.0)] or buffer alone (as a control) was microinjected into cytosol of Met-1 cells (transfected with HA-tagged NH₂-terminally truncated C1199 TiamlcDNA) using Micromanipulator 5171 and Transjector 5246 (Eppendorf, Germany). Twenty hours after injection, cells were fixed with 2% formaldehyde in phosphate-buffered saline for 1h and processed for immunocytochemical staining as described below.

Expression Constructs: Both the full-length mouse TiamlcDNA (FL1591) and the NH₂-terminally truncated TiamlcDNA (C1199) were kindly provided by Dr. John G. Collard (The Netherlands Cancer Institute, The Netherlands). Specifically, the full-length Tiam1 (FL1591) cDNA was cloned into the eukaryotic expression vectors, pMT2SM. The truncated C1199 Tiam1 cDNA [carring a hemagglutinin epitope (HA)-tag at the 3' end] was cloned in the eukaryotic expression vector, pUTSV1 (Eurogentec, Belgium). The deletion construct, HA-tagged C1199 Tiam1Δ717-727 (deleting the sequence between aa717 and aa727 of Tiam1) was derived from C1199 Tiam1 using QuikChange™ Site-Directed Mutagenesis Kit (Stratagene). Briefly, two complimentary mutagenic oligonucleotide primers containing the desired deletion (5'CCCAACCATCAACCAGGTGTTTGAGGGAATATTTGATG-3') was designed and synthesized. First, the cycling reaction utilizing 30ng double-stranded DNA template of C1199 Tiam1 plasmid and two complimentary primers was performed to produce mutated cDNA according to the manufacturer's instruction. Subsequently, 1 ul of the Dpn I restriction enzyme (10U/ul) was added directly to the cycling reaction products in order to digest the parental supercoiled double-stranded DNA. This Dpn I -treated cDNA was used to transform supercompetent cells (e.g. Epicurian Coli XL 1-Blue). Finally the deletion construct was confirmed by DNA sequencing.

Cell Transfection: To establish a transient expression system, cells (e.g. Met-1 cells or COS-7 cells) were transfected with various plasmid DNAs including TiamlcDNAs [e.g. the full-length mouse TiamlcDNA (FL1591) or HA -tagged NH₂-terminally truncated C1199 TiamlcDNA or HA-tagged C1199 Tiam1Δ717-727 (lacking the ankyrin-binding domain) cDNA or vector control constructs] using electroporation methods. Briefly, cells (e.g. COS-7 cells or Met-1 cells) were plated at a density of 1 x 10⁶ cells per 100 mm dish and were transfected with 25 µg/dish plasmid DNA using electroporation at 230v and 960 µFD with a Gene Pulser (Bio-Rad). Transfected cells were grown in the culture medium for at least 24-48h. Various transfectants were then analyzed for the expression of HA-tagged Tiam1 mutant proteins by anti-HA-mediated immunoblot, immunoprecipitation, immunostaining and functional assays as described below.

Double Immunofluorescence Staining: To detect intracellular localization of various regulatory molecules in membrane protrusions, Met-1 cells [transiently transfected with the full-length Tiam1 (FL1591) cDNA or HA-tagged N-terminally truncated C1199 Tiam1 cDNA or HA-tagged C1199 Tiam1Δ717-727 (lacking the ankyrin-binding domain) cDNA or vector alone] grown in the presence and absence of certain agents [e.g. two anti-CD44 antibodies (e.g. rat anti-CD44 antibody or rabbit anti-CD44v3 antibody) (50µg/ml) or microinjected with C3 toxin (50µg/ml)] were first washed with PBS [0.1M phosphate buffer (pH 7.5) and 150mM NaCl] buffer and fixed by 2% paraformaldehyde. Subsequently, cells were then rendered permeable by ethanol treatment and stained with rhodamine (Rh)-labeled mouse anti-HA IgG followed by fluorescein (FITC)-conjugated rabbit anti-ankyrin IgG or FITC-labeled rabbit anti-CD44v3 antibodies. To detect non-specific antibody binding, rhodamine-labeled cells were incubated with FITC-conjugated normal mouse IgG or normal rat IgG. No labeling was observed in such control samples. The fluorescein- and rhodamine-labeled samples were examined with a confocal laser scanning microscope (MultiProbe 2001 Inverted CLSM system,

Molecular Dynamics, Sunnyvale, CA).

Immunoprecipitation and Immunoblotting Techniques: Unlabeled or surface biotinylated cells were washed in 0.1M phosphate buffered saline (PBS; pH 7.2) and solubilized in RIPA buffer (11,12). Subsequently, the biotinylated cells were used for anti-CD44-mediated immunoprecipitation as described previously (24). These biotinylated materials precipitated by rat anti-CD44 antibody were analyzed by SDS-PAGE, transferred to the nitrocellulose filters and incubated with rabbit anti-CD44v3 antibody plus peroxidase-conjugated goat anti-rabbit IgG or ExtrAvidin-peroxidase (Sigma Co.). After an addition of peroxidase substrate (Pierce Co.), the blots were developed using ECL chemiluminescence reagent (Amersham Life Science, England) according to the manufacturers instructions.

In some cases, cells were then solubilized in 50 mM Tris-HCl (pH 7.4), 150 mM NaCl, and 1% Nonidet P-40 (NP-40) buffer followed by immunoprecipitation by rabbit anti-CD44v3 antibody. The immunoprecipitated material (or the whole cell lysate) was solubilized in SDS sample buffer and analyzed by SDS-PAGE (with 7.5% gel). Separated polypeptides were then transferred onto nitrocellulose filters. After blocking non-specific sites with 3% bovine serum albumin, the nitrocellulose filters were incubated with mouse anti-RhoA antibody (5µg/ml) plus peroxidase-conjugated goat anti-mouse IgG (1:10,000 dilution). The blots were developed using ECL chemiluminescence reagent (Amersham Life Science, England) according to the manufacturer's instructions.

In some experiments, Met-1 cells or COS cells [e.g. untransfected or transfected by various Tiam1 cDNAs including the full-length mouse Tiam1cDNA (FL1591) or HA-tagged NH₂-terminally truncated C1199 Tiam1cDNA or HA-tagged C1199 Tiam1Δ717-727 (lacking the ankyrin-binding domain) cDNA or vector only] were immunoblotted with rabbit anti-Tiam1 (5µg/ml) or mouse anti-HA antibody (5µg/ml) for 1h at room temperature followed by incubation with horseradish peroxidase-conjugated goat anti-rabbit IgG or goat anti-mouse IgG (1:10,000 dilution) at room temperature for 1 h. The blots were developed using ECL chemiluminescence reagent (Amersham Life Science, England) according to the manufacturers instructions.

To analyze GTP binding to RhoA, the anti-RhoA-immunoprecipitated materials were transferred to nitrocellulose membrane and probed with 0.25µM [³⁵S] GTPγS (1,250Ci/mmol) in the presence or in the absence of 100µM unlabeled GTPγS. The procedures for [³²P]ADP-ribosylation with botulinum toxin C3 were the same as described previously (47,48). The radioactively labeled bands were detected by fluorography.

GTPase Activity Assay: The GTPase activity was performed as described previously with the following modification (49,50). The CD44v_{3,8-10}-bound RhoA complex (20 pmole) (with or without C3-mediated ADP-ribosylation reaction) were incubated in the GTPase assay buffer [20mM Tris-HCl (pH 7.4), 5 mM MgCl₂, 0.1% cholate, and 1 mM dithiothreitol (DTT) in the presence of 1µM [γ-³²P]GTP (4 x 10⁴ cpm/pmole) and 0.1 mM ATP] in a reaction volume of 50µl at 4°C for 30min. The samples were then incubated at 37°C for various time intervals. Following incubation, 100µl of 1% BSA, 0.1% dextran sulfate made in 20mM phosphate buffer (pH 8.0) was added to the reaction mixtures followed by the addition of 750µl of activated charcoal suspension containing 20mM phosphate buffer (pH 8.0). Following incubation at 4°C for 30 min, the reaction mixtures were centrifuged, and ³²P_i released in the supernatant was determined by liquid scintillation counting. The results are expressed as pmole of P_i released per µg of protein. In control samples, the non-specific release of P_i caused by the background level of GTPase activity (associated with preimmune rabbit IgG-bead associated materials) was determined. The non-specific release of P_i in control samples was less than 10% of that released by RhoA complexed with CD44v_{3,8-10} samples and has been subtracted. Each assay was set up in triplicate and repeated at least 3 times. All data were analyzed statistically by Student's t test and statistical significance was set at p<0.01.

Binding Of ¹²⁵I-Labeled Ankyrin/Fodrin/Spectrin To Synthetic Peptides: Nitrocellulose discs (1 cm diameter) were coated with ≈ 1 µg of either the ankyrin-binding region peptide (GEGTDAVKRSL) or a scrambled peptide (GRATLEGSDKV)

(synthesized by Dr. Eric Smith, University of Miami). Following coating, the unoccupied sites on the discs were blocked by incubation with a solution containing 20 mM Tris-HCl (pH 7.4) and 0.3% bovine serum albumin at 4°C for 2 h. The discs were then incubated with ^{125}I -labeled ankyrin/spectrin/fodrin (≈ 3000 cpm/ng) at 4°C for 2 h in 1 ml binding buffer (20 mM Tris-HCl pH 7.4, 150 mM NaCl, 0.2 % bovine serum albumin). Following binding, the discs were washed three times in the binding buffer and the disc bound radioactivity was estimated. The non-specific binding was determined in the presence of a 100-fold excess of one of the respective unlabeled ligands and was subtracted from the total binding. Non-specific binding was approximately 30% of the total binding. As a further control, the ligands were also incubated with uncoated nitrocellulose discs to determine the binding observed due to the "stickyness" of various ligands. Nonspecific binding was observed in these controls.

Binding of ^{125}I -labeled Tiam1 To Ankyrin: Purified ^{125}I -labeled Tiam1 (≈ 0.32 nM protein, 1.5×10^4 cpm/ng) was incubated with 30 μl of ankyrin conjugated to sepharose beads (≈ 0.75 μg protein) in 0.5 ml of the binding buffer (described above). Binding was carried out in the presence or absence of various concentrations (10^{-10}M - 10^{-5}M) of unlabeled competing synthetic peptide (GEGTDAVKRSL-corresponding to the ankyrin binding sequence of Tiam1) at 4°C for 5 h under equilibrium conditions. Equilibrium conditions were determined by performing a time course (e.g. 1 h-10 h) of the binding reaction. Following binding, the beads were washed in the binding buffer and the bead bound radioactivity was determined. Non-specific binding was determined in the presence of either a 100 fold excess of unlabeled ankyrin or using bovine serum albumin conjugated sepharose beads. Non-specific binding was approximately 20-30% of the total binding, and was subtracted from the total binding.

Binding Of ^{125}I -Labeled Ankyrin To Tiam1 and Its Mutant Proteins: Aliquots (10-20 ng proteins) of both purified wild type (the full length Tiam1) and mutant proteins (e.g. C1199 Tiam1 or HA-tagged NH_2 -terminally truncated C1199 Tiam1 or HA-tagged C1199 Tiam1 Δ 717-727 (lacking the ankyrin-binding domain) bound to the anti-Tiam1 or anti-HA immunoaffinity beads were incubated with 0.5 ml of a binding buffer (20 mM Tris.HCl pH 7.4, 150 mM NaCl, 0.1% bovine serum albumin and 0.05% Triton X-100) in presence of various concentrations (10-400 ng/ml) of ^{125}I -labeled ankyrin (5,000 cpm/ng protein) at 4°C for 5 h. The non-specific binding was determined in presence of a 50-100 fold excess of unlabeled ankyrin and also by incubating the anti-Tiam1 or anti-HA immunobeads alone in the presence of same concentrations of ^{125}I -labeled ankyrin. Following binding, the immunobeads were washed extensively in binding buffer and the bead-bound radioactivity was estimated.

Tiam1-Mediated GDP/GTP Exchange For RhoA Proteins: Purified RhoA (isolated from Met-1 cells by mouse anti-RhoA antibody) or RhoA complexed with CD44v_{3,8-10} or *E. coli*-derived GST-tagged RhoA (20pmole) was preloaded with GDP (30 μM) or radioactively labeled [^3H]GDP (30 μM ; 11Ci/mmol) (or in the presence of 1mM unlabeled GDPyS) in 10 μl buffer containing 25mM Tris-HCl (pH 8.0), 1mM DTT, 4.7mM EDTA, 0.16mM MgCl_2 and 200 $\mu\text{g}/\text{ml}$ BSA at 37° for 7min. In order to terminate preloading procedures, additional MgCl_2 was then added to the solution (reaching a final concentration of 9.16mM) as described previously (38). Four μl of the preloaded RhoA GTPase was added to 16 μl of the exchange mixture containing 2 pmole of Tiam1 isolated from Met-1 cells or COS-7 cells transfected by various Tiam1 cDNAs [e.g. the full-length mouse Tiam1cDNA (FL1591) or HA-tagged NH_2 -terminally truncated C1199 Tiam1cDNA or HA-tagged C1199 Tiam1 Δ 717-727 (lacking the ankyrin-binding domain) cDNA or vector only], 1mM GTP and 60 $\mu\text{g}/\text{ml}$ BSA in exchanger buffer. At various time intervals (e.g. 0, 2, 4, 6, 8, 10, 20min, etc.), an aliquot of samples was analyzed as described previously (38). Under this condition, at least 90% of pre-loaded [^3H]GDP was released by the addition of EDTA. For measuring exchange reactions of $\text{GTP}\gamma^{35}\text{S}$ binding for RhoA GTPases, RhoA (e.g. Met-1 RhoA or GST-tagged RhoA) (20pmole) was preloaded with 0.5 μM GDP in exchange buffer containing 200 $\mu\text{g}/\text{ml}$ BSA. Subsequently, 2 pmole of Tiam1 [isolated from Met-1 transfectants or COS-7 transfectants) or vector-transfected cells/untransfected cells (control samples)] was preincubated for 10 min with

0.25 μ M GTP γ ³⁵S (1,250Ci/mmol) and 2.25 μ M GTP γ S (or in the presence of 1mM unlabeled GTP γ S) followed by adding GDP-loaded RhoA GTPases (e.g. Met-1 RhoA or GST-tagged RhoA). The amount of GTP γ ³⁵S bound to samples in the absence of GTPases was subtracted from the original values. Data represent an average of triplicates from 3-5 experiments. The standard deviation was less than 5%.

Tumor Cell Migration and Invasion Assays: Twenty-four transwell units were used for monitoring in vitro cell migration and invasion as described previously (24,51). Specifically, the 8 μ m porosity polycarbonate filters coated with the reconstituted basement membrane substance Matrigel (Collaborative Research, Lexington, MA) were used for the cell invasion assay (24,51). The 8 μ m porosity polycarbonate filters (without Matrigel coating) were used for the cell migration assay (24,51). Met-1 cells transfected with various Tiam1-related cDNAs [e.g. full-length Tiam1 cDNA or HA-tagged N-terminally truncated Tiam1 cDNA or HA-tagged Tiam1 deletion mutant (Tiam1 Δ 717-727) cDNA or vector alone] [$\approx 1 \times 10^4$ cells/well in phosphate buffered saline (PBS), pH 7.2] were placed in the upper chamber of the transwell unit. The growth medium containing high glucose DMEM supplemented by 10% fetal bovine serum were placed in the lower chamber of the transwell unit. After 18h incubation at 37°C in a humidified 95% air/5% CO₂ atmosphere, cells on the upper side of the filter were removed by wiping with a cotton swap. Cell migration and invasion processes were determined by measuring the cells that migrate to the lower side of the polycarbonate filters by standard cell number counting methods as described previously (24,51). Each assay was set up in triplicate and repeated at least 5 times. All data was analyzed statistically by Student's t test and statistical significance was set at $p < 0.01$.

RESULTS

(A) Physical Linkage Between CD44v_{3,8-10} and RhoA GTPase

The expression of CD44 variant isoforms is known to be closely correlated with metastatic and proliferative behavior of a variety of tumor cells including various carcinomas such as human breast tumor cells (5,46). To directly examine CD44 isoform expression on the surface of Met-1 cells [derived from a high metastatic potential tumor in transgenic mice expressing polyomavirus middle T oncogene (45) and shown to induce a high level of intratumoral microvessel formation (45)], we have utilized surface biotinylation techniques and a specific monoclonal rat anti-CD44 antibody that recognizes the CD44 epitope located at the N-terminus of the common domain of all CD44 isoforms (12,46). Our results indicate that a single surface-biotinylated polypeptide (M. W. \approx 260kDa) displaying immunological cross-reactivity with CD44 is preferentially expressed on the surface of Met-1 cells (Fig. 1, lane 1). This surface labeled 260kDa protein can also be immunoprecipitated by rat anti-CD44 antibody followed by immunoblotting (Fig. 1, lane 2) using rabbit anti-CD44v₃ antibody raised specifically against the v₃ sequence indicating that this protein is a CD44v₃-containing isoform. No CD44v₃-containing material is observed in control samples when either normal rat IgG or preimmune rabbit serum is used (Fig. 1, lane 3).

A previous study based on RT-PCR, Southern blot, cloning and nucleotide sequence analyses determined that the 260kDa CD44v₃-containing isoform expressed on the surface of Met-1 cells belongs to the CD44v_{3,8-10} isoform [containing v3 and v8-10 exon insertions into the standard form of CD44(CD44s)] (24). The 260kDa CD44v_{3,8-10} molecule has also been found to be closely associated with a matrix metalloproteinase (MMP-9), and to interact with the cytoskeleton during "invadopodia" formation and tumor cell migration in Met-1 cells (24). These findings suggest that CD44v_{3,8-10} and the associated cytoskeleton play an important role in metastatic tumor cell behavior (24). The rationale for our focusing on the interaction between small molecular weight GTPases and CD44v_{3,8-10}-cytoskeleton is based on a previous report by Tsukita and co-workers suggesting the involvement of CD44-associated cytoskeletal proteins (ERM) in Rho-induced cytoskeletal effects (52). Using a non-ionic detergent (NP-40) extraction (to isolate membrane-cytoskeleton complexes as shown previously) (24) of surface biotinylated Met-1 cells and anti-CD44v3-mediated immunoprecipitation, we have found that the 260kDa CD44v_{3,8-10} expressed on the cell surface is physically associated in a complex with a 25 kDa protein (Fig.

1, lane 4). Further analyses indicate that the 25kDa protein (Fig. 1, lane 4) shares immuno-cross reactivity with RhoA detected in Met-1 cells (Fig. 1, lane 5). These findings firmly establish the fact that CD44v_{3,8-10} and RhoA are closely associated with each other as a complex in vivo. We have also determined that the complex containing CD44v_{3,8-10} and RhoA can be dissociated by 0.6M NaCl treatment (data not shown).

Using an in vitro [³⁵S]GTPγS binding assay, we have determined that the 25kDa RhoA (complexed with CD44v_{3,8-10}) displays guanine nucleotide binding activity (Fig. 1, lane 6). In the presence of excess amounts of unlabeled GTPγS, no radioactive labeling was observed (Fig. 1, lane 7). Subsequently, we have found that the 25 kDa RhoA protein can be [³²P]ADP-ribosylated by C3 toxin (Fig. 1, lane 8). In a control sample, when [³²P]ADP-ribosylation of RhoA was carried out in the absence of C3 toxin, no labeling of RhoA was observed (Fig. 1, lane 9). Most importantly, C3-mediated ADP-ribosylation of RhoA complexed with CD44v_{3,8-10} eliminates more than 90% of the GTPase activity (Table 1). These data indicate that CD44v_{3,8-10}-bound RhoA has GTPase activity and also contains a site for ADP-ribosylation mediated by the RhoA inhibitor, C3 toxin.

(B) Identification of The Guanine Nucleotide Exchange Factor, Tiam1 (An Upstream Activator for RhoA GTPase) In Met-1 Cells

RhoA GTPase (e.g. RhoA and Rac) becomes activated when bound GDP is exchanged for GTP by a process catalysed by guanine nucleotide (GDP/GTP) exchange factors (GEFs) or GDP-dissociation stimulator (GDS) proteins [i.e. promoting GTP binding to RhoA by facilitating the release of GDP] (31,34,35). Tiam1 (T-lymphoma invasion and metastasis 1) is a GEF and contains a Dbl homology (DH) domain and an adjacent pleckstrin homology (PH) domain which are commonly detected in most GEFs (34,36). The unique feature of Tiam1 is its additional PH domain and a Discs-large homology region (DHR) in the N-terminal part of the protein (37).

A Tiam1 transcript has previously been detected in breast cancer cells (33). In this study we have analyzed Tiam1 expression (at the protein level) in breast tumor cells such as Met-1 cell line. Immunoblot analysis, utilizing anti-Tiam1 antibody designed to recognize the specific epitope located at the C-terminus of Tiam1 molecule, reveals a single polypeptide (M. W. ≈ 200kDa) (Fig. 2, lane 1). This 200kDa Tiam1-like molecule expressed in Met-1 cells is very similar to the Tiam1 detected in COS-7 cells which were transiently transfected with the full-length Tiam1 cDNA (Fig. 2, lane 2) or with the vector alone (Fig. 2, lane 3-revealing a low level of endogenous Tiam1). We believe that Tiam1 detected in Met-1 cells or COS-7 transfectants revealed by anti-Tiam1-mediated immunoblot is specific since no protein is detected in these cells in the presence of preimmune rabbit IgG (Fig. 2, lane 4-6).

To confirm that the Tiam1-like molecule functions as a GDP/GTP exchange factor [or a GDP-dissociation stimulator (GDS) protein] for RhoA (purified from Met-1 cells or *E. coli*-derived GST-RhoA), we have isolated Tiam1 from Met-1 cells using anti-Tiam1-conjugated Sepharose beads. First, RhoA (Met-1RhoA or GST-RhoA) was preloaded with [³H]GDP followed by an incubation with Tiam1 isolated from Met-1 cells. As shown in Fig. 3A, Met-1's Tiam1 induces a rapid release of [³H]GDP from both Met-1 RhoA and GST-RhoA (Fig. 3A-indicated by solid lines) within the first 2-3 min of the reaction. The [³H]GDP release detected in the reaction is greatly reduced if the [³H]GDP-preloaded RhoA proteins were incubated in the presence of an excess amount of unlabeled GTPγS (Fig. 3A-indicated by dotted lines). In addition, we have found that Tiam1 isolated from Met-1 cells induces the exchange of preloaded unlabeled GDP for [³⁵S]GTPγS on RhoA (e.g. Met-1 RhoA or GST-RhoA) in a time-dependent manner (Fig. 3B-indicated by solid lines). For example, the initial onset of the exchange reaction occurs within 2-3 min after the addition of Tiam1 (Fig. 3B-indicated by solid lines). The reaction reaches its maximal level approximately 10min after Tiam1 treatment (Fig. 3B-indicated by solid lines), followed by a rapid decrease of GDT/GTP exchange capability (≈20 min after Tiam1 addition) (Fig. 3B-indicated by solid lines). In the presence of a large excess of unlabeled GTPγS, the amount of [³⁵S]GTPγS associated with RhoA is significantly decreased (Fig. 3B-indicated by dotted lines). Our data indicate that both the

exchange rate and the total amount of bound [35 S]GTP γ S on Met-1 RhoA and GST-RhoA are very similar (Fig. 3B-indicated by solid lines). Further analysis induces that the ability of Tiam1 isolated from Met-1 cells (Fig. 3C-a) to promote GDP/GTP exchange on RhoA is identical to that carried out by Tiam1 isolated from COS-7 transfected with the full-length Tiam1 cDNA (Fig. 3C-b) or N-terminally truncated C1199 Tiam1 cDNA (Fig. 3C-c). In control samples (using vector-transfected COS cells), the amount of [35 S]GTP γ S binding to GST-RhoA is significantly reduced (Fig. 3C-d). Therefore, we believe that Tiam1 of Met-1 cells definitely functions as a GDP/GTP exchange factor or GDS protein for RhoA GTPase.

(C) Interaction of Tiam 1 and the Cytoskeletal Proteins, Ankyrin

Certain cytoskeleton proteins, such as ankyrin, are known to be involved in regulating a variety of cellular activities (6, 53). Using an *in vitro* binding assay, we have found that 125 I-labeled ankyrin binds Tiam1 (isolated from Met-1 cells) specifically (Fig. 4B-a). In the presence of an excess amount of unlabeled ankyrin, the binding between ankyrin and Tiam1 is greatly reduced (Fig. 4B-b). Protein sequence analyses show that Tiam1 contains the sequence " 717 GEGTDAVKRS 727 L" (in mouse), or " 717 GEGTEAVKRS 727 L" (in human) (Fig. 5A) which shares a great deal of sequence homology with the ankyrin binding domain of the cell adhesion receptor, CD44 family (Fig. 5B). To test whether the sequence "GEGTDAVKRSL" of Tiam 1 protein is in fact involved in ankyrin binding, we have examined the ability of an 11 amino acid synthetic peptide, identical to "GEGTDAVKRSL", to bind various cytoskeletal proteins. As shown in Table 2, this synthetic peptide binds specifically to ankyrin, but not other cytoskeletal proteins such as fodrin or spectrin. A control peptide, containing the scrambled sequence (GRATLEGSDKV) with the same amino acid composition as that of the synthetic peptide, does not bind to any cytoskeletal proteins tested (e.g. ankyrin, fodrin and spectrin) (Table 2). Furthermore, the 11 a.a. synthetic peptide (GEGTDAVKRSL) competes effectively for the ankyrin binding site on purified Met-1 Tiam1 molecule with an apparent inhibition constants (K_i) of ≈ 0.5 nM (Fig. 4A). These findings strongly suggest that the amino acid sequence, "GEGTDAVKRSL", is an essential part of the ankyrin binding domain of the Tiam 1 molecule in breast tumor cells (Met-1 cells).

Most importantly, we have found that the binding of ankyrin to Tiam 1 (isolated from Met-1 cells) significantly increases the GDP-GTP exchange activity of RhoA GTPases (Fig. 6A and 6B). Therefore, we believe that the unique 11 a.a. region "GGVGDVLRKPS" is important not only for ankyrin binding to Tiam 1, but it also plays a pivotal role in the up-regulation of Tiam 1-mediated GDP-GTP exchange activity of GTPases during cytoskeleton action.

(D) Effect of Tiam1 or Its Deletion Mutant (Lacking An Ankyrin-Binding Domain) On Tumor Cell Invasion and Migration

Previous studies indicate that the invasive phenotype of tumor cells characterized by an "invadopodia" structure (or membranous projections) (54,55) and tumor cell migration (28,29) is closely associated with CD44 $v_{3,8-10}$ -linked cytoskeletal function (24). In this study we have found that overexpression of Tiam1 [by transfecting Met-1 cells with HA-tagged N-terminally truncated C1199 Tiam1 cDNA (Fig.7 A-F) or the full-length Tiam1cDNA (data not shown)] promotes membrane motility. Specifically, we have observed that HA-tagged C1199 Tiam1 (Fig. 7A and 7D) is co-localized with ankyrin (Fig. 7B and 7C) and CD44 (e.g. CD44 $v_{3,8-10}$) (Fig. 7E and 7F) in long, extended membrane spikes or in certain membrane ruffling regions (indicated by arrow heads). In contrast, ankyrin-associated membrane projections are significantly reduced in vector-transfected Met-1 cells (Fig. 7b and 7c). No HA staining is detected in these control samples (Fig. 7a). In addition, we have demonstrated that Met-1 cells transfected with C1199 Tiam1cDNA up-regulates tumor cell invasion and migration as compared to Met-1 cells transfected with vector alone (Table 3). These results are consistent with previous findings indicating that transfection of NIH3T3 cells with the N-terminally truncated C1199 Tiam1 cDNA confers potent oncogenic properties (32).

Tiam1 is known to activate several Rho-like GTPase including RhoA, Rac1

and Cdc42 (25). One way to determine which Rho-like GTPases are directly involved in Tiam1-mediated membrane motility in Met-1 cells is to utilize specific Rho inhibitors. For example, RhoA (but not Rac and Cdc42) is a substrate for certain bacterial toxins such as Clostridium botulinum C3 toxin (47,48). The fact that C3 toxin ADP-ribosylates RhoA (but not Rac and Cdc42) (Fig. 1, lane 8) and thereby inactivates RhoA GTPase (isolated from CD44v_{3,8-10} containing materials) (Table 1) suggests that the RhoAGTPase is one of the major Rho-like GTPases associated with CD44v_{3,8-10} in metastatic Met-1 cells. Moreover, microinjection of C3 toxin into Met-1 cells transfected with HA-tagged N-terminally truncated C1199 Tiam1 cDNA causes cell shape change and blocks membrane motility by inhibiting Tiam1 (Fig. 7d) association with ankyrin in the plasma membrane (Fig. 7e and 7f). Together, these findings suggest that Tiam1 is involved in activating RhoA-specific signaling required for cytoskeleton-associated membrane motility in Met-1 cells.

Treatment of Met-1 cells (e.g. untransfected cells or C1199 Tiam1 cDNA-transfected cells or vector-transfected cells) with various anti-CD44 antibodies [e.g. rat anti-CD44 antibody (recognizes a common determinant of all CD44 isoforms) or rabbit anti-CD44v3 antibody (specific for v3 sequence)] also causes a significant inhibition of Tiam1 (Fig. 7g) and CD44-associated membrane motility (Fig. 7h and 7i), tumor cell invasion and migration (Table 3). These observations suggest that Tiam1 function and CD44v3 signaling are closely coupled.

Finally, we have constructed a HA-tagged C1199 Tiam1 deletion mutant lacking the ankyrin binding site (designated as C1199 Tiam1Δ717-727) (Fig. 8A). The truncated C1199 Tiam1Δ717-727 cDNA and the wild-type C1199 Tiam1 were then transiently transfected into Met-1 cells, respectively. Our results indicate that both the C1199 Tiam1Δ717-727 mutant (Fig. 8B, lane 3) and the wild-type C1199 Tiam1 (Fig. 8B-lane2) are expressed as a 160 kDa polypeptide in Met-1 transfectants by immunoblot using anti-HA antibody. No protein band was detected in vector-transfected Met-1 cells (Fig. 8B, lane 1). Further analyses using anti-HA-conjugated immuno-beads indicate that the HA-tagged C1199 Tiam1Δ717-727 mutant protein (isolated from Met-1 transfectants) displays a drastic reduction (approximately ~90-95% inhibition) in ankyrin-binding (Fig. 8C-c) compared to the HA-tagged wild-type C1199 Tiam1 (Fig. 8C-b). No ankyrin binding is observed in materials associated with anti-HA-beads isolated from vector-transfected cells (Fig. 8C-a). The C1199 Tiam1Δ717-727 mutant protein also displays a significant loss (~90% reduction) in its ability to induce GDP/GTP exchange reaction by RhoA (Fig. 8D) as compared to the wild-type C1199 Tiam1 (Fig. 8D). Addition of ankyrin to the wild-type C1199 Tiam1 stimulates both the rate of exchange and the total amount of GDP/GTP exchange for RhoA (Fig. 8D); whereas the C1199 Tiam1Δ717-727 mutant protein fails to respond to ankyrin-induced guanine nucleotide exchange activity (Fig. 8D). These results further support the notion that the 11aa sequence between aa717 and 727 of Tiam1 molecule is an ankyrin-binding domain which is required for the regulation of Tiam1's GDP-GTP exchange function.

Most importantly, we have found that overexpression of C1199 Tiam1Δ717-727 mutant (by transfecting Met-1 cells with C1199 Tiam1Δ717-727 cDNA) abolishes Tiam1 (Fig. 7i) association with ankyrin (Fig. 7k and 7l) in the cell membrane. In fact, this Tiam1 mutant protein (Fig. 7G) facilitates CD44-mediated cell-cell adhesion (Fig. 7H and 7I). The C1199 Tiam1Δ717-727 mutant also functions as a potent dominant-negative form of Tiam1 which effectively represses various metastatic tumor cell behaviors including tumor cell invasion and migration (Table 3) as compared to those observed in the wild-type C1199 Tiam1 cDNA-transfected Met-1 transfectants (Table 3). These findings strongly suggest that the ankyrin binding site located within Tiam1 plays an important role in RhoA activation leading to ankyrin and CD44v_{3,8-10}-associated cytoskeleton functions during breast tumor cell progression.

(7) CONCLUSIONS

The expression of CD44 variant isoforms has been found to be closely associated with invasive and metastatic behaviors of breast carcinoma cells (5,46). In particular, the CD44v3-containing isoforms (e.g. CD44v_{3,8-10}) are detected preferentially on highly malignant breast carcinoma tissues and, in fact, there is a direct correlation between CD44v3 isoform expression and increased histologic grade of the malignancy (46,56). One study indicates that expression of the CD44v3 isoform in breast tumors may be used as an accurate predictor of overall survival (45,57). It has been speculated that some of these CD44v3 isoforms on epithelial cells may act as surface modulators to facilitate unwanted growth factor receptor-growth factor interactions (13,14) and subsequent tumor formation. It is also possible that these CD44 variants may activate the cytoskeleton which leads to abnormal tumor cell-specific phenotypes (e.g. tumor cell invasion and migration) and metastatic breast cancer progression.

Recently, we have found that the CD44v3 isoform, CD44v_{3,8-10}, is expressed as a 260kDa polypeptide in breast tumor cells (Met-1 cell line-derived from a high metastatic potential tumor in transgenic mice expressing polyomavirus middle T oncogene) (45). This CD44v_{3,8-10} isoform is closely associated with the matrix metalloproteinase, MMP-9, and interacts directly with the cytoskeleton to promote tumor cell-specific phenotypes including tumor cell invasion and migration (24). These findings suggest that CD44v_{3,8-10} and the associated cytoskeleton play an important role in metastatic tumor cell behavior (24). Dissection of the transmembrane pathways controlling CD44v_{3,8-10}-associated cytoskeletal activities should aid in understanding the intracellular events underlying breast tumor cell invasion and metastasis.

Changes in cytoskeletal function and organization have been linked to the activation of Rho-like proteins, including RhoA, Rac1 and Cdc42 (25), during cellular motility in a number of cell types (e.g. epithelial cells, fibroblasts and neuronal cells) (32,33,39-41,58-60). Tsukita and his co-workers have shown that CD44 interacts with certain cytoskeletal proteins [e.g. ezrin, radixin and moesin (ERM)] which bind to F-actin (61,62). This CD44-ERM-F-actin complex appears to be an essential prerequisite for the Rho GTPase-induced cytoskeletal changes (22,61,62). Our current data indicate that RhoA (but not Rac or Cdc42) is closely associated with CD44v_{3,8-10} as a complex in Met-1 cells (Fig. 1). Moreover, CD44v_{3,8-10} complexed with RhoA activates Rho-kinase (ROK) which is required for CD44v_{3,8-10}-specific cytoskeleton function and metastatic behaviors in Met-1 cells (30). Consequently, it is important to determine the upstream activator(s) of RhoAGTPase during CD44v_{3,8-10}-related oncogenic signaling.

We have focused on guanine nucleotide exchange factors (GEFs) (the Dbp or DH family) such as Tiam1 in this study because these GEFs have oncogenic capability and they function as upstream activators of RhoA signaling (31,38-41). In Met-1 cells, Tiam1 is an approximately 200 kD protein which is similar to that described in other cell types (Fig. 2). Tiam1 isolated from Met-1 cells is indeed capable of carrying out GDP/GTP exchange for RhoA. *in vitro* (Fig. 3). Sequence analysis of Tiam1 suggests that its association with the invasive and metastatic phenotype is mediated via membrane-linked cytoskeletal regulation and/or activation of Rho family GTPases (32-41). Based on mutational analyses and immunofluorescence staining, Collard and his co-workers report that the NH2-terminus PH domain is required for Rac-dependent membrane ruffling and C-Jun NH2-terminal kinase activation in fibroblasts and COS cells (63). Between the N-terminal PH domain and the DH domain is a region with sequence homology to the Discs-large homologous region (DHR) of the Drosophila tumor suppressor protein (37). Although its function is unknown, this region may facilitate interaction with the membrane-linked cytoskeleton (38-41).

Ankyrin, one of the most important membrane-linked cytoskeletal proteins, is known to bind to a number of plasma membrane-associated proteins including band 3, two other members of the anion exchange gene family (53), Na⁺/K⁺-ATPase (62,63), the amiloride-sensitive Na⁺ channel (64), the voltage-dependent Na⁺ channel (65), Ca²⁺ channels (66-68) and the adhesion molecule, CD44 (6). It has been suggested that the binding of ankyrin to certain membrane-associated

molecules may be necessary for signal transduction, cell adhesion, cell migration and tumor metastasis (5-7,53).

The cytoplasmic domain of CD44 (approximately 70 a. a. long) is highly conserved ($\geq 90\%$) in most of the CD44 isoforms, and is clearly involved in specific ankyrin binding (20,21). The ankyrin-binding domain of CD44 has also been mapped using deletion mutation analyses and mammalian expression systems (20,21). In particular, the ankyrin-binding domain [e.g. "NGGNGTVEDRKPSSEL" between aa 306 and aa320 in the mouse CD44 (20) and "NSGNGAVEDRKPSGL" aa304 and aa318 in human CD44 (21)] is required for cell adhesion (20,21), the recruitment of Src kinase and the onset of tumor cell transformation (21). Recent data indicate that the amino acid sequence-"NGGNGTVEDRKPSSEL" [located between aa480 and aa494 of CD44v_{3,8-10}] in Met-1 cells also binds specifically to the cytoskeletal protein, ankyrin (but not fodrin or spectrin), and belongs to the ankyrin-binding domain of CD44v_{3,8-10} (24).

The structural homology between the ankyrin binding domain of the Tiam1 protein (the sequence between aa717 and aa727) and the CD44 family is quite striking (Fig. 5). The fact that (a) a peptide containing the sequence (⁷¹⁷GEGTDAVKRS⁷²⁷L) of Tiam1 can directly bind ankyrin but not fodrin or spectrin (Table 2); (b) a Tiam1 peptide (aa717-727) peptide competes with Tiam1 for binding to ankyrin (Fig. 4); and (c) the Tiam1 deletion mutant protein (e.g. C1199 Tiam1Δ717-727-lacking the ankyrin-binding site) fails to bind ankyrin (Fig. 8C) and displays a significantly reduced GDP/GTP exchange activity (in the presence or absence of ankyrin treatment) (Fig. 8D) strongly suggests that the sequence (⁷¹⁷GEGTDAVKRS⁷²⁷L) of Tiam1 is directly involved in ankyrin binding and ankyrin-induced stimulation of Tiam1-catalyzed GDP-GTP exchange activity for RhoA. Therefore, the putative ankyrin binding site in Tiam1 (aa717-aa727) which resides between the N-terminal PH domain and DHR domain as the "regulatory domain" is required for the up-regulation of the GDP/GTP exchange activity of RhoAGTPases such as RhoA. Preliminary data indicate that ankyrin acts as a linker molecule between Tiam1 and CD44. The upstream activator(s) or signal(s) required for stimulating ankyrin-Tiam1 interaction with CD44 is currently undergoing investigation.

Using double immunocytochemical staining and confocal microscopic analyses, we have shown that transfection of Met-1 cells with HA-tagged N-terminally truncated C1199 Tiam1 cDNA stimulates Tiam1 (Fig. 7A and 7D) co-localization with ankyrin (Fig. 7B and 7C) and CD44v_{3,8-10} (Fig. 7E and 7F) in membrane motility-related events (e.g. membrane ruffling or spike formation) as well as tumor cell invasion and migration (Table 3). These Tiam1-activated oncogenic responses are consistent with previous studies indicating Tiam-activated Rho-like GTPases may act as downstream effectors of Ras in both tumorigenesis and progression to metastatic diseases (32,33). In fibroblasts, Tiam1-induced membrane ruffling is independent of RhoA activity (69). In fact, Rac1 acts downstream of Tiam1 signaling during the function of certain cell adhesion molecules such as the laminin receptor, α6β1 integrin (60).

In this study we have found that RhoAGTPase complexed with CD44v_{3,8-10} can be modified and inhibited by C3 toxin (Fig. 1, lane 8). Tiam1-induced CD44v_{3,8-10} membrane motility is also effectively inhibited by C3 toxin (Fig. 7d-f). These results suggest that Tiam1-catalysed RhoA activation is closely involved in CD44v_{3,8-10}-associated cytoskeleton function. In nerve cells, Tiam1 is involved in regulating both Rac1- and RhoA-mediated pathways during neurite formation (60). Apparently, the balanced between two Rho-like GTPases (e.g. Rac1 and RhoA) determines neuronal morphology (60). The question whether Tiam1-Rac1 signaling is also involved in breast tumor progression remains to be addressed.

In epithelial Madin-Darby canine kidney (MDCK) cells, Tiam1-Rac signaling up-regulates E-cadherin-mediated adhesion and plays an invasion-suppressor role in Ras-transformed MDCK cells (59). The different responses by Tiam1-catalysed Rho-like GTPases (e.g. Rac1 or RhoA) in various cell types may be controlled by selective upstream signaling [e.g. availability of certain activators including cytoskeletal proteins (e.g. ankyrin), cell adhesion receptors (e.g. CD44, integrin or E-cadherin), growth activators (e.g. LPA, PDGF or serum) or

extracellular matrix components, etc.] which may result in selective GTPase activation. For example, our data demonstrate that overexpression of the ankyrin-deletion mutant of Tiam1 by transfecting Met-1 cells with C1199 Tiam1 Δ 717-727 cDNA results in a reversal of metastatic tumor cell-specific phenotypes (Fig. 7G-7I; Table 3). In particular, the loss of membrane spikes and ruffling structures accompanied by a CD44-mediated cell-cell adhesion in the C1199 Tiam1 Δ 717-727 expressing cells (Fig. 7G-7I) is consistent with previous mutation analyses suggesting the need for the N-terminal PH and its adjacent region including the sequence of aa717 and aa727 in Tiam1 function (63). Finally, our data indicate that tumor cell-specific behaviors (e.g. membrane motility, tumor cell invasion and migration) can also be inhibited by rat anti-CD44 antibody (recognizes a common determinant of all CD44 isoforms) or rabbit anti-CD44v3 antibody (recognizes v3-specific sequence) (Table 3). These findings suggest that oncogenic signaling (derived from the v3-coded structure of CD44v_{3,8-10}) and ankyrin binding to Tiam1 play a pivotal role in RhoA activation required for cytoskeleton function and CD44v_{3,8-10}-specific tumor cell behaviors during metastatic breast tumor cell progression.

(8) REFERENCES

1. Trowbridge, I.S., Lesley, J., Schulte, R., Hyman, R., and Trotter, J. (1982) *Immunogenetics* **15**,299-312.
2. Omary, M.B., Trowbridge, I.S., Letarte, M., Kagnoff, M.F., and Isacke, C.M. (1988) *Immunogenetics*. **27**,460-464.
3. Bourguignon, L.Y.W., Lokeshwar, V.B., He, J., Chen, X., and Bourguignon, G. J. (1992) *Mol. Cell. Biol.* **12**,4464-4471.
4. Brown, T., Bouchard, T., St. John, T., Wayner, E., and Carter, W.G. (1991) *J. Cell Biol.* **113**,207-221.
5. Bourguignon, L.Y.W., Iida, N., Welsh, C.F., Zhu, D., Krongrad, A., and Pasquale, D. (1995) *J. Neuro-Oncol.* **26**,201-208.
6. Bourguignon, L.Y.W. (1996) *Current Topics in Membranes* (Ed: W.J. Nelson) **43**,293-312.
7. Bourguignon, L.Y.W., Zhu, D., and Zhu, H.B. (1998) *Frontiers in Bioscience* **3**,637-649.
8. Screaton, G.R., Bell, M.V., Jackson, D.G., Cornelis, F.B., Gerth, U., and Bell, J.I. (1992) *Proc. Natl. Acad. Sci. (USA)* **89**,12160-12164.
9. Lesley, J., Hyman, R., and Kincade, P. (1993) *Adv. Immunol.* **54**,271-235.
10. Goldstein, L.A., Zhou, D.F.H., Picker, L.J., Minty, C.N., Bargatze, R.F., Ding, J.F., and Butcher, E.C. (1989) *Cell* **56**,1063-1072.
11. Lokeshwar, V.B. and Bourguignon, L.Y.W. (1991) *J. Biol. Chem.* **266**,17983-17989.
12. Lokeshwar, V.B., Iida, N., and Bourguignon, L.Y.W. (1996) *J. Biol. Chem.* **271**,23853-13864.
13. Bennett, K., Jackson, D., Simon, J., Tanczos, E., Peach, R., Modrell, B., and Stamenkovic, I. (1995) *J. Cell Biol.* **128**,687-698.
14. Jackson, D.G., Bell, J.I., Dickinson, R., Timans, J., Shields, J. and Whittle, N. (1995) *J Cell Biol* **128**,673-685.
15. Bourguignon, L.Y.W., Walker, G., Suchard, S., and Balazovich, K. (1986) *J. Cell Biol.* **102**,2115-2124.
16. Kalomiris, E.L., and Bourguignon, L.Y.W. (1988) *J. Cell Biol.* **106**,319-327.
17. Kalomiris, E.L. and Bourguignon, L.Y.W. (1989) *J. Biol. Chem.* **264**,8113-8119.
18. Bourguignon, L.Y.W., Kalomiris, E. and Lokeshwar, V.B. (1991) *J. Biol. Chem.* **266**,11761-11765.
19. Lokeshwar, V.B. and Bourguignon, L.W.B. (1992) *J. Biol. Chem.* **267**,22073-22078.
20. Lokeshwar, V.B., Fregien, N., and Bourguignon, L.Y.W. (1994) *J. Cell Biol.* **126**,1099-1109.
21. Zhu, D. and Bourguignon, L.Y.W. (1998) *Cell Motility and the Cytoskeleton* **39**:209-222.

22. Tsukita, S., Yonemura, S. and Tsukita, S. (1997) *Curr. Opin. Cell Biol.* **9**,70-75.
- 23 Bourguignon, L.Y.W., Zhu, H., Chu, A., Iida, N., Zhang, L. and Hung, H.C. (1997) *J. Biol. Chem.* **272**, 27913-27918.
24. Bourguignon, L.Y.W., Gunja-Smith, Z., Iida, N., Zhu, H.B., Young, L.J.T., Muller, W.J. and Cardiff, R.D. (1998) *J. Cell. Physiol.* **176**,206-215.
25. Hall, A. (1998) *Science* **279**,509-514.
26. Narumiya, S. (1996) *J. Biochem.* **120**,215-228.
27. Dickson, R.B., and Lippman, M.E. (1995) *The Molecular Basis of Cancer* (Mendelsohn, J., Howlwy, P.M., and Israel, M.A. and Liotta, L.A., ed.), W.B. Saunders Company, Philadelphia, PA, pp. 358-359.
28. Jiang, W. G., Puntis, M. C. A., and Hallett, M. B. (1994) *British J. Surgery* **81**,1576-1590.
29. Lauffenburger, D.A. and Horwitz, A. F. (1996) *Cell* **84**,359-369.
30. Bourguignon, L.Y.W., Zhu, H.B., Shao, L., and Zhu, D. (1998) submitted to *J. Exp. Med.*
31. Van Aelst, L., and D'Souza-Schorey, C. (1997) *Genes Dev.* **11**,2295-2322.
32. Habets, G.G.M., Scholtes, E.H.M., Zuydgeest, D., van der Kammen, R.A., Stam, J.C., Berns, A., and Collard, J.C. (1994) *Cell* **77**,537-549.
33. Habets, G.G.M., van der Kammen, R.A., Stam, J.C., Michiels, F., and Collard, J.C. (1995) *Oncogene* **10**,1371-1376.
34. Hart, M.J., Eva, A., Evans, T., Aaronson, S. A., and Cerione, R.A. (1991) *Nature* **354**,311-314.
35. Hart, M.J., Eva, A., Zangrilli, D., Aaronson, S. A., Evans, T., Cerione, R.A., and Zheng, Y. (1994) *J. Biol. Chem.* **269**,62-65.
36. Lemmon, M.A., Ferguson, K.M., and Schlessinger, J. (1996) *Cell* **85**,621-624.
37. Pontings, C.P. and Phillips, C. (1995) *Trends Biochem. Sci.* **20**,102-103.
38. Michiels, F., Habets, G.G.M., Stam, J.C., van der Kammen, R.A., and Collard, J. C. (1995) *Nature* **375**,338-340.
39. Ridley, A.J., and Hall, A. (1992) *Cell* **70**,389-399.
40. Ridley, A.J., Paterson, H.F., Johnston, C.L., Diekman, D., and Hall, A. (1992) *Cell* **70**, 401-410.
41. Nobes, C.D. and Hall, A. (1995) *Cell* **81**,53-62.
42. Fleming, I.N., Elliott, C.M., Collard, J.G., and Exton, J.H. (1997) *J. Biol. Chem.* **272**,33105-33110.
43. Fleming, I.N., Elliott, C.M. and Exton, J.H. (1998) *FEBS Lett* **429**,229-233.
44. Michiels, F., Stam, J.C., Hordijk, P.L., van der kammen, R.A., Ruuls-Van Stalle, L., Feltkamp, C.A., and Collard, J.G. (1997) *J. Cell Biol.* **137**,387-398.
45. Cheung, A.T.W., Young, L.J.T., Chen, P.C.Y., Chao, C.Y., Ndoeye, A., Barry, P.A., Muller, W.J., and Cardiff, R.D. (1997) *Int. J. Oncology* **11**,69-77.
46. Iida, N., and Bourguignon, L.Y.W. (1995) *J Cell Physiol.* **162**,127-133.
47. Ohashi, Y., and Narumiya, S. (1987) *J. Biol. Chem.* **262**,1430-1433.
48. Aktories, K., Weller, U., and Chhatwal, G. S. (1987) *FEBS Lett* **212**,109-113.
49. Kabcenell, A.K., Goud, B., Northup, J. K., and Novick, P.J. (1990) *J. Biol. Chem.* **265**,9366-9372.
50. O'Neil, L. A. J., Bird, T.A., Gearing, A.J.H., and Saklatvala, J. (1990) *J. Biol. Chem.* **265**,3146-3152.
51. Merzak, A., Koochekpour, S., and Pilkington, G.J. (1994) *Cancer Res.* **54**,3988-3992.
52. Hirao, M., Sato, N., Kondo, T., Yonemura, S., Monden, M., Sasaki, T., Takai, Y., Tsukita, S., and Tsukita, S. (1996) *J. Cell Biol.* **135**,36-51.
53. Bennet, V. (1992). Ankyrins. *J. Biol. Chem.* **267**,8703-8706.
54. Monsky, W.L., Lin, C.Y. and Chen, W.T. (1994) *Cancer. Res.* **54**,5702-5710.
55. Mueller, S.C. and Chen, W.T. (1991) *J. Cell Sci.* **99**,213-225.
56. H.P. Sinn, Heider, K.H., Skroch-Angel, P., von Minckwitz, G., Kaufmann, M., Herrlich, P. and Ponta, H. (1995) *Cancer Res. and Treatment* **36**,307-313.
57. M. Kaufmann, Heider, K.H., Sinn, H.P., von Minckwitz, G., Ponta, H. and Herrlich, P. (1995) *Lancet* **345**,615-619.

58. Stam, J.C., Michiels, F., van der Kammen, R.A., Moolenaar, W.H., and Collard, J.G. (1998) *EMBO* **17**,4066-4074.
59. Hordijk, P.L., ten Klooster, J.P., van der Kammen, R.A., Michiels, F., Oomen, L.C., and Collard, J.G. (1998) *Science* **278**,1464-1466.
60. Leeuwen, F.N., Kain, H.E., Kammen, R.A., Michiels, F., Kranenburg, O.W., and Collard, J.G. (1997) *J. Cell Biol.* **139**,797-807.
61. Tsukita, S., Oishi, K., Sato, N., Sagara, I., Kawai, A., and Tsukita, S. (1994) *J. Cell Biol.* **126**,391-401.
62. Hirao, M., Sato, N., Kondo, T., Yonemura, S., Monden, T., Sasaki, T., Takai, Y., Tsukita, S., and Tsukita, S. (1996) *J. Cell Biol.* **135**,36-51.
63. Michiels, F., Stam, J.C., Hordijk, P.L., van der Kammen, R.A. Ruuls-Van Stalle, L. Feltkamp, C.A., and Collard, J.G. (1997) *J. Cell Biol.* **137**,387-398.
62. Nelson, W. J., and Veshnock, P. J. (1987) *Nature (Lond)*. **328**,533-536.
63. Morrow, J.S., Cianci, C.D., Ardito, A.S., and Kashgarian, M. (1989). *J. Cell Biol.* **108**,455-465.
64. Smith, P.R., Saccomani, G., Joe, E.H., Angelides, K.J., and Benos, D.J. (1991) *Proc. Natl. Acad. Sci. (USA)* **88**,6971-6975.
65. Kordeli, E., Lambert, S., and Bennet, V. (1995) *J. Biol. Chem.* **270**,2352-2359.
66. Bourguignon, L.Y.W., Chu, A., Jin, H., and Brandt, N.R. (1995) *J. Biol. Chem.* **270**,17917-17922.
67. Bourguignon, L.Y.W., and Jin, H., (1995) *J. Biol. Chem.* **270**,7257-7260.
68. Bourguignon, L.Y.W., Jin, H., Iida, N., Brandt, N., and Zhang, S. H. (1993) *J. Biol. Chem.* **268**,7290-7297.
69. Nishiyama, T., Sasaki, T., Takaishi, K., Kato, M., Yaku, M., Araki, K., Matsuura, Y., and Takai, Y. (1994) *Mol. Cell Biol.* **14**,2447-2456.

(9) APPENDICES

Table 1: GTPase activity assay of RhoA complexed with CD44v_{3,8-10}.

Treatment	P _i Release (cpm x 10 ³)
No Treatment	650
C3 toxin-treated	62

Aliquots of RhoA complexed with CD44v_{3,8-10} (as described in Fig.1) (20 pmole) were incubated with 1 μ M [γ -³²P]GTP (4 x 10⁴ cpm/pmole). The amount of ³²P_i liberated was determined as described under Materials and Methods. Data represent an average of triplicates. The standard deviation was less than 5%.

Table 2: Binding of ¹²⁵I-labeled cytoskeletal proteins (e.g ankyrin, spectrin and fodrin) to synthetic peptides.

A: Binding To "GEGTDAVKRSL" (The sequence between aa717 and aa727 of Tiam1):

	(nM x CPM Bound)
¹²⁵ I-labeled Ankyrin	15,000 \pm 125
¹²⁵ I-labeled Spectrin	850 \pm 35
¹²⁵ I-labeled Fodrin	1,040 \pm 30

B: Binding To "GRATLEGSDKV" (The scrambled sequence):

	(nM x CPM Bound)
¹²⁵ I-labeled Ankyrin	1,020 \pm 36
¹²⁵ I-labeled Spectrin	956 \pm 28
¹²⁵ I-labeled Fodrin	1,157 \pm 46

¹²⁵I-labeled cytoskeletal proteins [e.g ankyrin (100ng), spectrin (100ng) and fodrin (100ng)] were incubated with nitrocellulose discs coated with either the synthetic peptide "GEGTDAVKRSL" (corresponding to the sequence between aa717 and aa727 of Tiam1) or the scrambled peptide "GRATLEGSDKV" at 4°C for 4h as described in the Materials and Methods. Non-specific binding was determined in the presence of a 100-fold excess of the respective unlabeled cytoskeletal proteins and subtracted from the total binding.

Table 3: Measurement of Tumor Cell Invasion and Migration.

A: In vitro cell invasion:

Cells	<u>Cell Invasion^a</u> (% of Control) ^b		
	Preimmune serum treated	Rabbit anti-CD44v3-treated	Rat anti-CD44-treated
Untransfected cells (control)	100	27	24
Vector-transfected cells	98	25	22
C1199 Tiam1cDNA-transfected cells	149	56	43
C1199 Tiam1 Δ 717-727cDNA transfected cells	20	≤ 5	≤ 5

B: In vitro cell migration:

Cells	<u>Cell Migration^a</u> (% of Control) ^b		
	Preimmune serum-treated	Rabbit anti-CD44v3-treated	Rat anti-CD44-treated
Untransfected cells (control)	100	25	21
Vector-transfected cells	95	25	23
C1199 Tiam1cDNA-transfected cells	155	52	49
C1199 Tiam1 Δ 717-727cDNA transfected cells	23	≤ 5	≤ 5

a: Met-1 cells [$\approx 1 \times 10^4$ cells/well in phosphate buffered saline (PBS), pH 7.2] [in the presence or absence of rat anti-CD44 antibody (50 μ g/ml) or rabbit anti-CD44v3 antibody (50 μ g/ml) or preimmune rabbit serum or normal mouse IgG (50 μ g/ml)] were placed in the upper chamber of the transwell unit. In some cases, Met-1 cells were transfected with either HA-tagged C1199 Tiam1 cDNA or HA-tagged C1199 Tiam1 Δ 717-727cDNA or vector alone. After 18h incubation at 37°C in a humidified 95% air/5% CO₂ atmosphere, cells on the upper side of the filter were removed by wiping with a cotton swap. Cell invasion and migration processes were determined by measuring the cells that migrate to the lower side of the polycarbonate filters by standard cell number counting methods as described previously (51). Each assay was set up in triplicate and repeated at least 3 times. All data were analyzed statistically by Student's t test and statistical significance was set at $p < 0.01$. In these experiments ≈ 30 to 40% of input cells ($\approx 1 \times 10^4$ cells/well) undergo in vitro cell invasion and migration in the control samples.

b: The values expressed in this table represent an average of triplicate determinations of 3-5 experiments with a standard deviation less than $\pm 5\%$.

FIGURE LEGEND

Fig. 1: Analysis of CD44v_{3,8-10} expression and CD44v_{3,8-10}-RhoA complex in mouse breast tumor cells (Met-1 cells).

Met-1 cells (5×10^5 cells) were solubilized by 1% Nonidet P-40 (NP-40) buffer followed by immunoblot and/or immunoprecipitation by anti-CD44 antibodies (e. g. rat anti-CD44 or rabbit anti-CD44v3) or mouse anti-RhoA. The immunoprecipitated material was then treated with SDS sample buffer and analyzed by SDS-PAGE. The procedures for identifying RhoA by [³⁵S]GTPγS binding or botulinum toxin C3-mediated [³²P]ADP-ribosylation were described in the Materials and Methods.

Lane 1: Immunoprecipitation of surface biotinylated Met-1 cells using monoclonal rat anti-CD44 antibody (recognizing CD44 epitope located at the N-terminus of the common domain of all CD44 isoforms) followed by ExtrAvidin-peroxidase reaction..

Lane 2: Immunoblot of rat anti-CD44-immunoprecipitated materials (obtained from lane 1) with rabbit anti-CD44v₃-specific antibody.

Lane 3: Immunoblot of Met-1 cells with preimmune rabbit serum.

Lane 4: Identification of biotinylated CD44v_{3,8-10} by ExtrAvidin-peroxidase and RhoA detection by mouse anti-RhoA-immunoblot in rabbit anti-CD44v3-immunoprecipitated materials.

Lane 5: Detection of RhoA in the whole cell lysate of Met-1 cells by anti-RhoA-mediated immunoblot.

Lane 6: Autoradiogram of [³⁵S]GTPγS binding (in the absence of unlabeled GTPγS) to RhoA obtained from anti-CD44v3-mediated immunoprecipitated materials.

Lane 7: Autoradiogram of [³⁵S]GTPγS binding (in the presence of unlabeled GTPγS) to RhoA obtained from anti-CD44v3-mediated immunoprecipitated materials.

Lane 8: Autoradiogram of [³²P]ADP-ribosylation of RhoA obtained from anti-CD44v3-mediated immunoprecipitated materials in the presence of botulinum toxin C3.

Lane 9: Autoradiogram of [³²P]ADP-ribosylation of RhoA obtained from anti-CD44v3-mediated immunoprecipitated materials in the absence of botulinum toxin C3.

Fig. 2: Detection of Tiam1 expression in Met-1 cells or COS-7 Transfectants.

Met-1 cells and COS-7 cells [transfected with the full-length Tiam1cDNA (FL1591) or vector alone] were solubilized in SDS sample buffer and analyzed by SDS-PAGE and immunoblot as described in the Materials and Methods.

Lane 1: Anti-Tiam1-mediated immunoblot of Met-1 cells.

Lane 2: Anti-Tiam1-mediated immunoblot of COS-7 cells transfected with the full-length Tiam1cDNA (FL1591).

Lane 3: Anti-Tiam1-mediated immunoblot of COS-7 cells transfected with vector alone.

Lane 4: Immunoblot of Met-1 cells with preimmune rabbit serum.

Lane 5: Immunoblot of COS-7 cells [transfected with the full-length Tiam1cDNA (FL1591)] with preimmune rabbit serum.

Lane 6: Immunoblot of COS-7 cells [transfected with vector alone] with preimmune rabbit serum.

Fig. 3: Tiam1-mediated GDP/GTP exchange for RhoA proteins.

Purified RhoA (complexed with CD44v_{3,8-10}) or *E. coli*-derived GST-tagged RhoA (20pmole) preloaded with radioactively labeled [³H]GDP (in the absence or presence of GTPγS) was added to the exchange mixture containing Tiam1 [isolated from Met-1 cells or COS-7 cells transfected by the full-length mouse Tiam1cDNA (FL1591) or the N-terminally truncated Tiam1 (C1199) cDNA] as described in the Materials and Methods. At various time intervals (e.g. 0, 2, 4, 6, 8, 10, 20 min, etc.), an aliquot of samples was analyzed as described previously (38). Under this condition, at least 90% of pre-loaded [³H]GDP was released by the addition of EDTA. For measuring exchange reactions of GTPγ³⁵S binding for RhoA GTPases, RhoA (e.g. Met-1 RhoA or GST-tagged RhoA) was preloaded with GDP. Subsequently, Tiam1 [isolated from Met-1 cells or COS-7 cells transfected with the full-length mouse Tiam1 cDNA (FL1591) or the N-terminally truncated Tiam1 (C1199) cDNA] was preincubated for 10 min with 0.25μM GTPγ³⁵S (1,250Ci/mmol) and 2.25μM GTPγS (or in the presence of 1mM unlabeled GTPγS) followed by adding GDP-loaded RhoA GTPases (e.g. Met-1 RhoA or GST-tagged RhoA). The amount of GTPγ³⁵S bound to

samples in the absence of GTPases was subtracted from the original values. Data represent an average of triplicates from 3-5 experiments. The standard deviation was less than 5%.

A: Dissociation of [^3H]GDP from Met-1 RhoA (Δ , solid line) or GST-RhoA (\bullet , solid line) in the presence of Tiam1 (isolated from Met-1 cells); and the amount of [^3H]GDP dissociated from Met-1 RhoA (Δ , dotted line) or GST-RhoA (\bullet , dotted line) in the presence of Tiam1 (isolated from Met-1 cells) plus 1mM GTPyS.

B: Kinetics of GTPyS bound to GDP-loaded Met-1 RhoA (Δ , solid line) or GST-RhoA (\bullet , solid line) in the presence of Tiam1 (isolated from Met-1 cells); and the amount of GTPyS associated with Met-1 RhoA (Δ , dotted line) or GST-RhoA (\bullet , dotted line) in the presence of Tiam1 (isolated from Met-1 cells) plus 1mM GTPyS.

C: The amount of GTPyS bound to GST-RhoA in the presence of Met-1 Tiam1(a) or the full-length Tiam1 (1591) isolated from COS-7 transfectants (b) or the C1199 Tiam1 isolated from COS-7 transfectants (c) or Tiam1 isolated from vector-transfected COS-7 cells (d).

Fig. 4: Binding interaction between Tiam1 and the cytoskeletal protein, ankyrin.

A: ^{125}I -labeled Tiam1 was incubated with ankyrin in the presence of various concentrations of unlabeled synthetic peptide (GEGTDAVKRSL) corresponding to the ankyrin-binding domain of Tiam1 as described in the Materials and Methods. The specific binding observed in the absence of any of the competing peptides is designated as 100%. The results represent an average of duplicate determinations for each concentration of the competing peptide used.

B: Tiam1 (isolated from Met-1 cells) bound to the anti-Tiam1 immuno-beads were incubated with ^{125}I -labeled ankyrin (5,000 cpm/ng protein) in the absence (a) or the presence (b) of 100 fold excess of unlabeled ankyrin. Following binding, the immunobeads were washed extensively in binding buffer and the bead-bound radioactivity was estimated.

Fig. 5: Sequence homology of the Ankyrin Binding Domain (ABD) located in Tiam1 and CD44.

A: Tiam1 contains a number of functional domains (e.g. M, the potential site for the attachment of a myristoyl group; P, PEST sequences; PHn, the N-terminal pleckstrin homology domain; ABD, ankyrin-binding domain; DHR, discs-large homology domain; DH, dbl-homology domain and PHc, the C-terminal pleckstrin homology domain).

B: CD44 contains several functional domains [e.g. extracellular adhesion domain, transmembrane domain, and an ankyrin-binding domain (ABD) located in the cytoplasmic side of the molecule].

Fig. 6: Stimulation of Tiam1-catalysed GDP/GTP exchange activity by ankyrin.

The amount of GTPyS bound to GDP-loaded GST-RhoA by Tiam1 (isolated from Met-1 cells) in the absence (A) or the presence (B) of ankyrin treatment.

Fig. 7: Double immunofluorescence staining of HA-tagged Tiam1 and CD44-cytoskeleton-associated molecules in Met-1 cells [transfected with HA-tagged C1199 Tiam1cDNA or HA-tagged C1199 Tiam1 Δ 717-727 cDNA].

To detect intracellular localization of various regulatory molecules in membrane protrusions, Met-1 cells [transiently transfected with HA-tagged N-terminally truncated C1199 Tiam1 cDNA or HA-tagged C1199 Tiam1 Δ 717-727 (lacking the ankyrin-binding domain) cDNA or vector alone] grown in the presence and absence of certain agents [e.g. two anti-CD44 antibodies (e.g. rat anti-CD44 antibody or rabbit anti-CD44v3 antibody) (50 $\mu\text{g}/\text{ml}$) or microinjected with C3 toxin (50 $\mu\text{g}/\text{ml}$)] were fixed by 2% paraformaldehyde. Subsequently, cells were rendered permeable by ethanol treatment and stained with rhodamine (Rh)-labeled anti-HA IgG followed by fluorescein (FITC)-conjugated anti-ankyrin IgG or FITC-labeled anti-CD44 antibodies. To detect non-specific antibody binding, rhodamine-labeled cells were incubated with FITC-conjugated normal mouse IgG or normal rat IgG or preimmune rabbit serum. No labeling was observed in such control samples.

A-C: Staining of HA-tagged C1199 Tiam1 (A) and ankyrin (B) were recorded separately. The merged image in yellow from (A) and (B) represents co-localization of Tiam1 and ankyrin (C) in Met-1 cells (transfected with C1199Tiam1 cDNA followed by staining with rhodamine-conjugated anti-HA antibody

and FITC-conjugated anti-ankyrin antibody, respectively) (Numerous membrane spikes and ruffling structures were indicated by arrow heads).

[a-c: Staining of non-specific materials (a) and ankyrin (b) were recorded separately. The merged image from (a) and (b) reveals only ankyrin staining (c) in Met-1 cells (transfected with vector alone followed by staining with rhodamine-conjugated anti-HA antibody and FITC-conjugated anti-ankyrin antibody, respectively).

[d-f: Staining of HA-tagged C1199 Tiam1 (d) and ankyrin (e) were recorded separately. The merged image from (d) and (e) reveals no significant co-localization of Tiam1 and ankyrin (f) in Met-1 cells (transfected with C1199 Tiam1 cDNA followed by microinjection with C3 toxin and staining with rhodamine-conjugated anti-HA antibody and FITC-conjugated anti-ankyrin antibody, respectively).

D-F: Staining of HA-tagged C1199 Tiam1 (D) and CD44 (E) were recorded separately. The merged image in yellow represents co-localization of Tiam1 and CD44 (F) in Met-1 cells (transfected with C1199Tiam1 cDNA followed by staining with rhodamine-conjugated anti-HA antibody and FITC-conjugated anti-CD44 antibody, respectively) (Numerous membrane spikes and ruffling structures were indicated by arrow heads).

[g-i: Staining of HA-tagged C1199 Tiam1 (g) and CD44 (h) were recorded separately. The merged image in yellow represents co-localization of Tiam1 and CD44 (i) in Met-1 cells (transfected with C1199Tiam1 cDNA) and incubated in the presence of rabbit anti-CD44v3 antibody followed by staining with rhodamine-conjugated anti-HA antibody and FITC-conjugated rat anti-CD44 antibody, respectively).

G-I: Staining of HA-tagged C1199Tiam1 Δ 717-727 (G) and CD44 (H) were recorded separately. The merged image in yellow represents little co-localization of Tiam1 and CD44 (I) in Met-1 cells (transfected with C1199Tiam1 Δ 717-727 cDNA followed by staining with rhodamine-conjugated anti-HA antibody and FITC-conjugated anti-CD44 antibody, respectively).

[j-l: Staining of HA-tagged C1199Tiam1 Δ 717-727 (j) and ankyrin (k) were recorded separately. The merged image in yellow represents little co-localization of Tiam1 and ankyrin (l) in Met-1 cells (transfected with C1199Tiam1 Δ 717-727 cDNA followed by staining with rhodamine-conjugated anti-HA antibody and FITC-conjugated anti-ankyrin antibody, respectively).

Fig. 8: Characterization of HA-tagged C1199 Tiam1 and its ankyrin-deletion mutant protein (e.g. HA-tagged C1199Tiam1 Δ 717-727).

A: Schematic illustration of the in vitro mutagenesis approach used in this study.

Both C1199 Tiam1 [the wild-type with no deletion of ankyrin-binding domain (ABD)] (a) and C1199Tiam1 Δ 717-727 [lacking the ankyrin-binding domain (ABD)] (b) were constructed according to the strategy described in the "Materials and Methods".

B: Anti-HA-mediated Immunoblot of Met-1 cells transiently transfected with vector alone (lane 1) or HA-tagged C1199 Tiam1 cDNA (lane 2) or HA-tagged C1199Tiam1 Δ 717-727 cDNA (lane 3).

C: The amount of ¹²⁵I-ankyrin binding to anti-HA immunoprecipitated materials isolated from Met-1 cells transfected with vector alone (a), or HA-tagged C1199Tiam1 cDNA (b) or HA-tagged C1199Tiam1 Δ 717-727 cDNA (c).

D: Kinetics of GTP³⁵S bound to GDP-loaded GST-RhoA in the presence of Tiam1 isolated from Met-1 cells [transfected with vector alone (▲), or HA-tagged C1199Tiam1 cDNA in the absence (◊) or the presence (◆) of ankyrin stimulation or HA-tagged C1199Tiam1 Δ 717-727 cDNA in the absence (◊) or the presence (●) of ankyrin stimulation].

Fig. 1

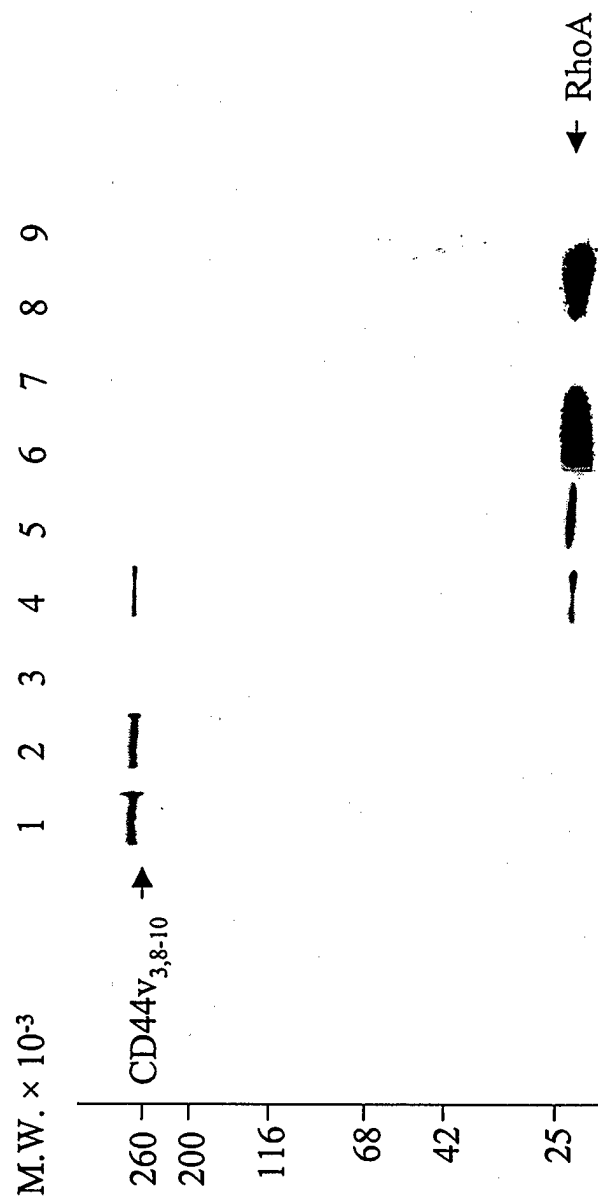


Fig. 2

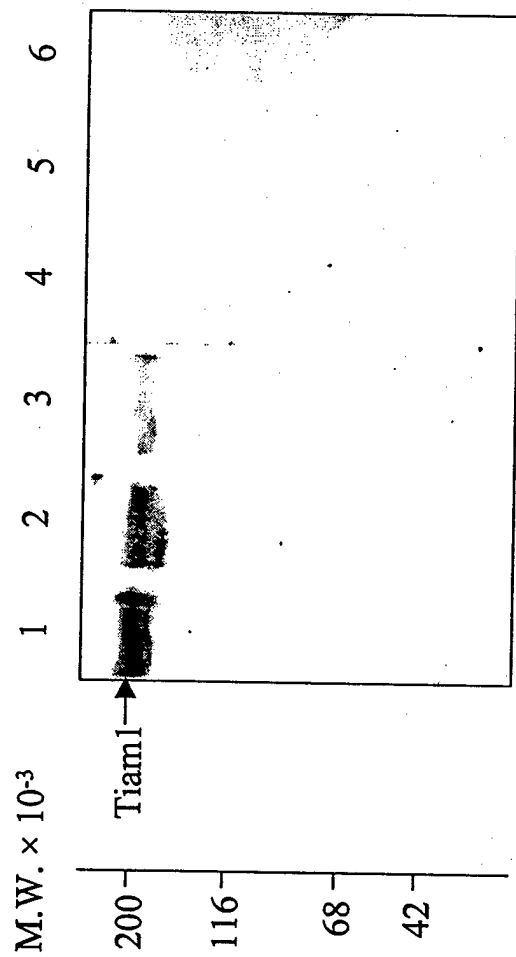


Fig. 3

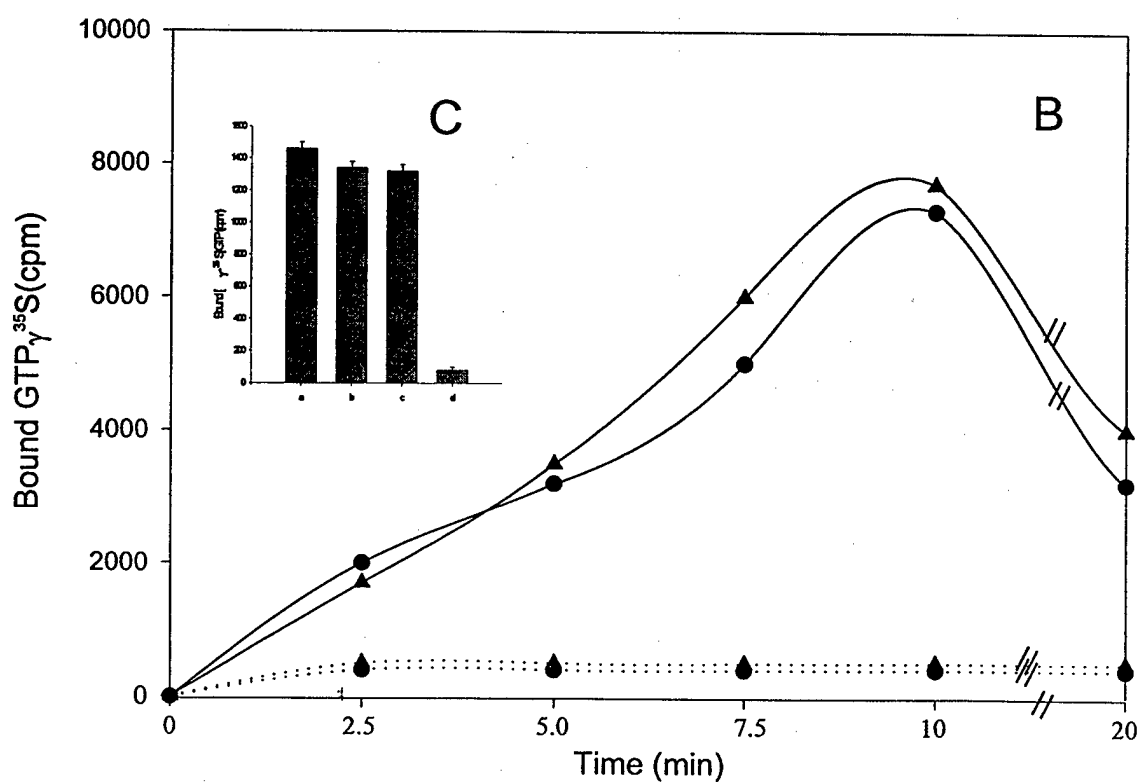
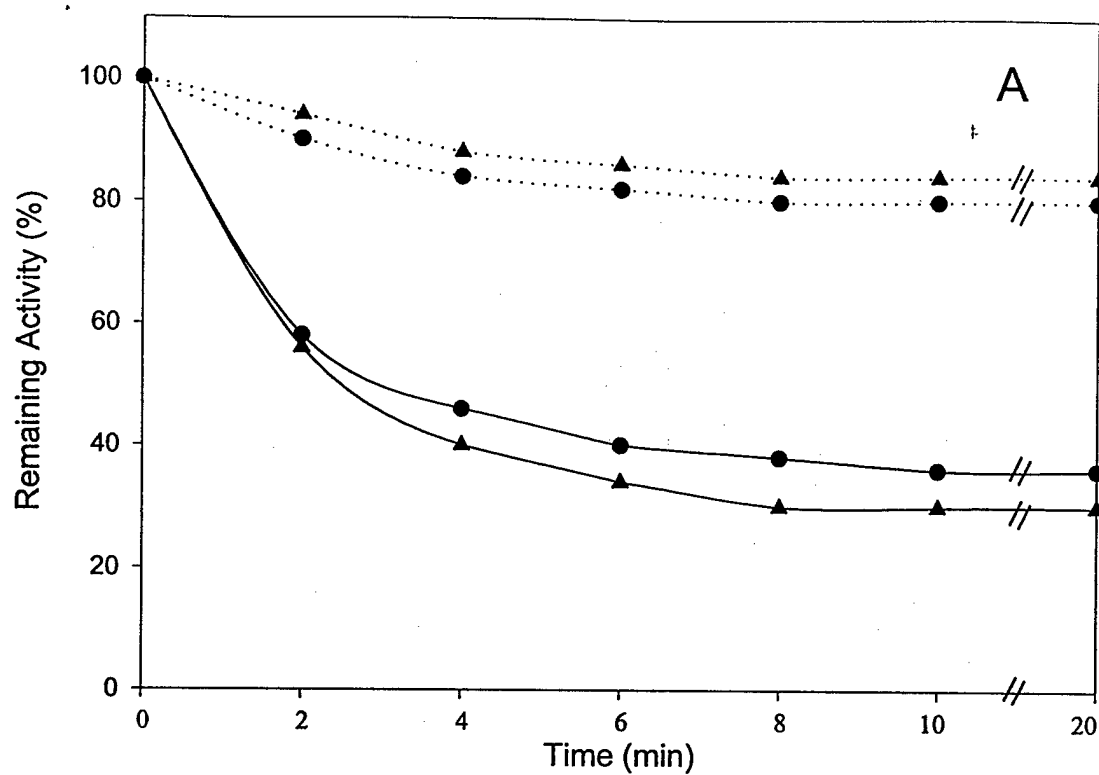


Fig. 4

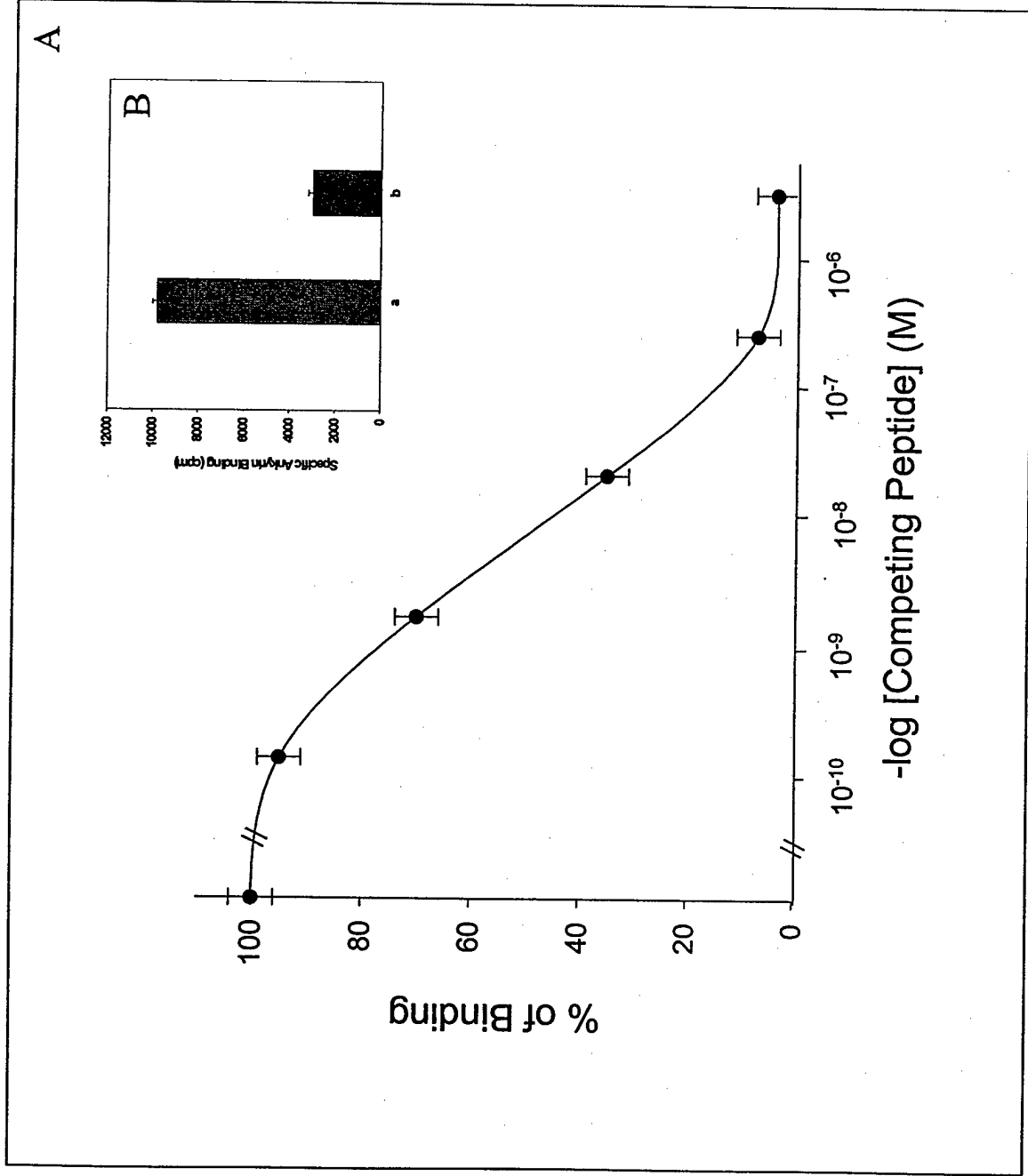


Fig. 5

Ankyrin Binding Domain (ABD)

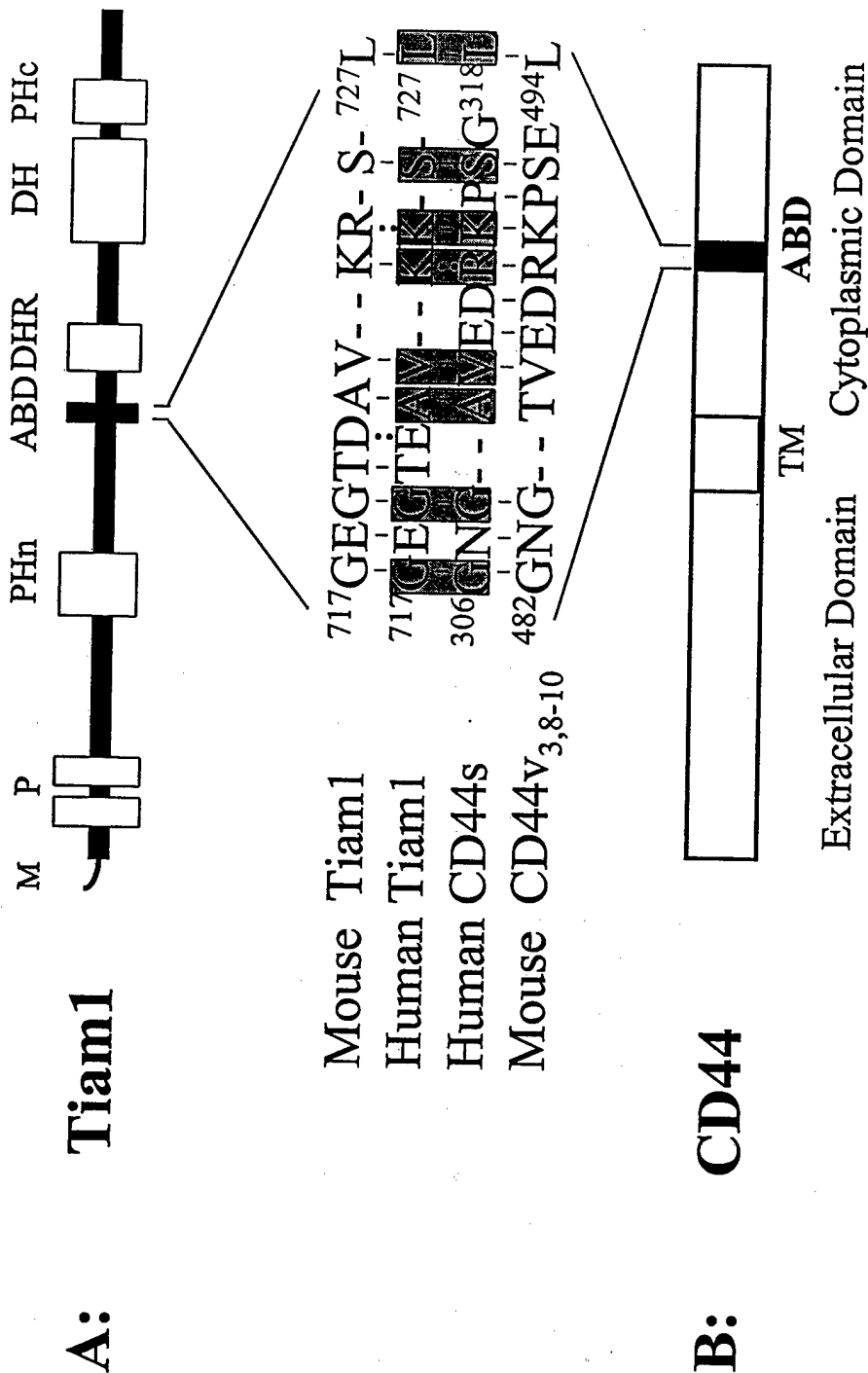
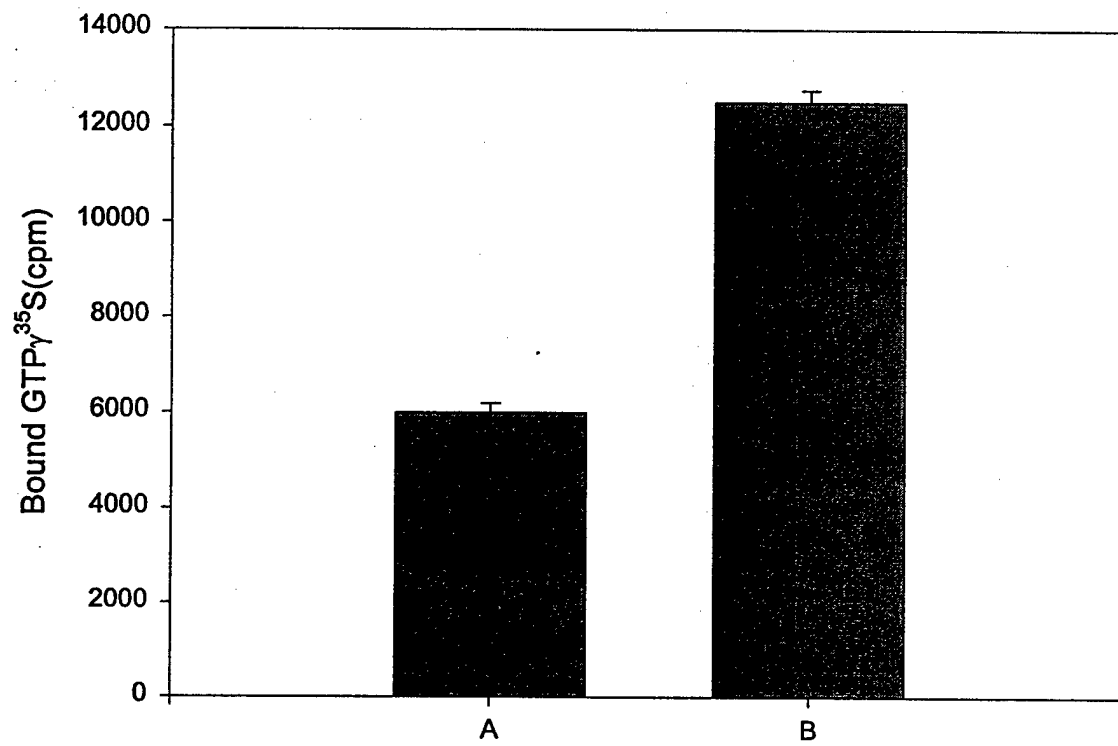


Fig. 6



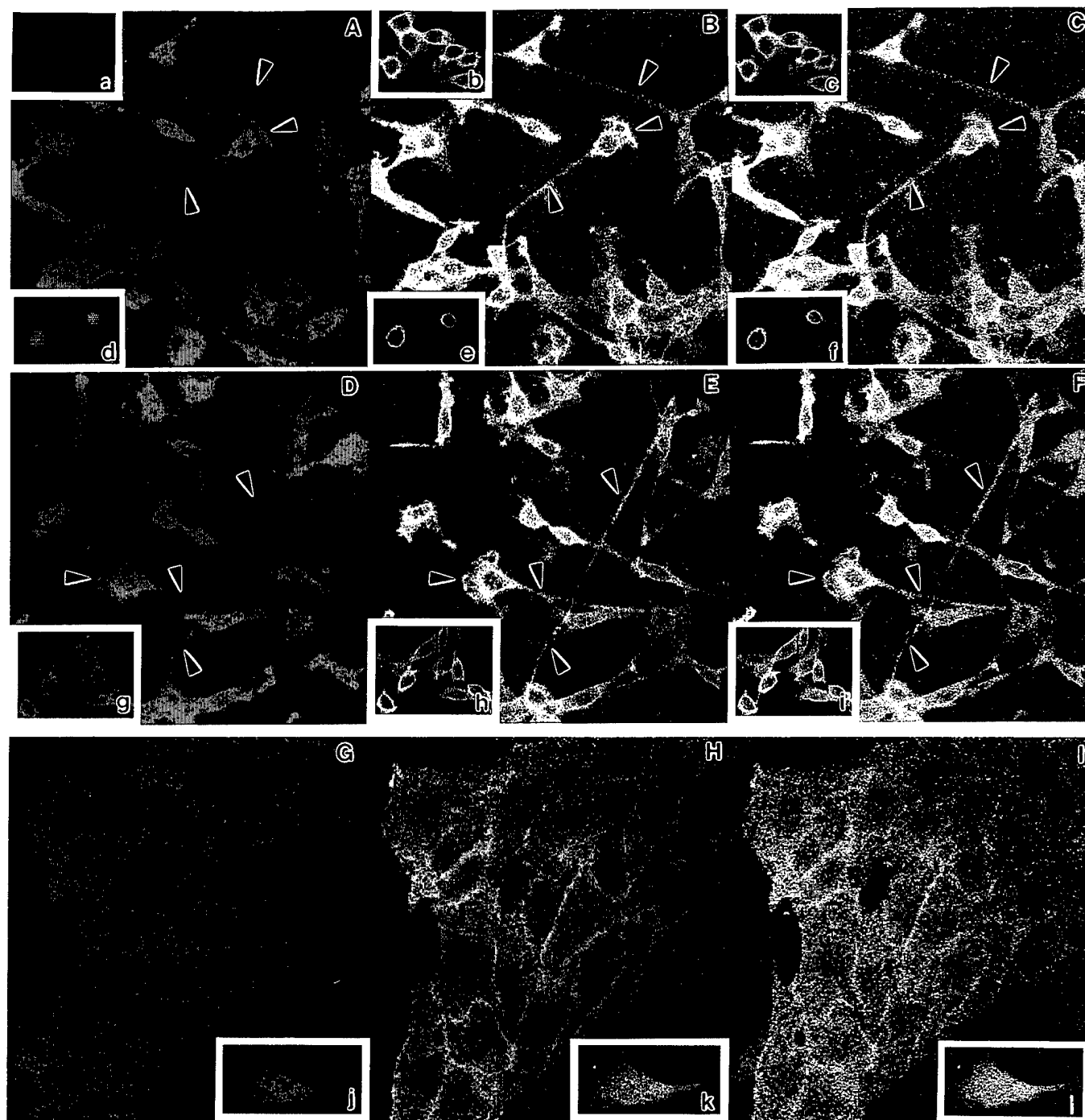


Fig. 8

